



HAL
open science

Embedment of Liposomes into Chitosan Physical Hydrogel for the Delayed Release of Antibiotics or Anaesthetics, and its First ESEM Characterization

S. Peers, P. Alcouffe, A. Montembault, C. Ladavière

► **To cite this version:**

S. Peers, P. Alcouffe, A. Montembault, C. Ladavière. Embedment of Liposomes into Chitosan Physical Hydrogel for the Delayed Release of Antibiotics or Anaesthetics, and its First ESEM Characterization. *Carbohydrate Polymers*, 2019, pp.115532. 10.1016/j.carbpol.2019.115532 . hal-02354077

HAL Id: hal-02354077

<https://hal.science/hal-02354077>

Submitted on 14 Dec 2020

HAL is a multi-disciplinary open access archive for the deposit and dissemination of scientific research documents, whether they are published or not. The documents may come from teaching and research institutions in France or abroad, or from public or private research centers.

L'archive ouverte pluridisciplinaire **HAL**, est destinée au dépôt et à la diffusion de documents scientifiques de niveau recherche, publiés ou non, émanant des établissements d'enseignement et de recherche français ou étrangers, des laboratoires publics ou privés.

Manuscript Number: CARBPOL-D-19-02967R2

Title: Embedment of Liposomes into Chitosan Physical Hydrogel for the Delayed Release of Antibiotics or Anaesthetics, and its First ESEM Characterization

Article Type: Research Paper

Keywords: Chitosan; physical hydrogels; liposomes; drug delivery systems; rifampicin; lidocaine

Corresponding Author: Dr. Catherine LADAVIERE, Ph.D.

Corresponding Author's Institution: CNRS

First Author: Soline PEERS, Ph.D.

Order of Authors: Soline PEERS, Ph.D.; Pierre ALCOUFFE; Alexandra MONTEBAULT, Ph.D.; Catherine LADAVIERE, Ph.D.

Abstract: This work describes the characterization of an original liposomes/hydrogel assembly, and its application as a delayed-release system of antibiotics and anaesthetics. This system corresponds to drug-loaded liposomes entrapped within a chitosan (CS) physical hydrogel. To this end, a suspension of pre-formed 1,2-dipalmitoyl-sn-glycero-3-phosphocoline liposomes loaded with an antibiotic (rifampicin, RIF), an anaesthetic (lidocaine, LID), or a model fluorescent molecule (carboxyfluorescein, CF), was added to a CS solution. The CS gelation was subsequently carried out without any trace of chemical cross-linking agent or organic solvent in the final system. Liposomes within the resulting gelled CS matrix were characterized for the first time by environmental scanning electron microscopy. The release of drugs from the assembly was investigated by fluorescence or UV spectroscopy. The cumulative release profiles of RIF and LID (and also CF for comparison) were found to be lower from the "drug-in-liposomes-in-hydrogel" (DLH) assembly in comparison to "drug-in-hydrogel" (DH) system.

Embedment of Liposomes into Chitosan Physical Hydrogel for the Delayed Release of Antibiotics or Anaesthetics, and its First ESEM Characterization

S. Peers, P. Alcouffe, A. Montembault*, C. Ladavière*

Lyon 1 University, UMR CNRS 5223, IMP, 15 boulevard André Latarjet, 69622 Villeurbanne Cedex, France

* Corresponding authors: alexandra.clayer-montembault@univ-lyon1.fr (A. Montembault), catherine.ladaviere@univ-lyon1.fr (C. Ladavière)

Highlights

- An original liposomes/chitosan hydrogel assembly was prepared by using a reproducible process.
- An antibiotic (rifampicin) or an anaesthetic (lidocaine) were pre-loaded in liposomes.
- **The resulting liposomes/chitosan hydrogel assembly was characterized** for the first time by environmental scanning electron microscopy (ESEM).
- The concept of delayed-release for rifampicin or lidocaine was demonstrated.

Embedment of Liposomes into Chitosan Physical Hydrogel for the Delayed Release of Antibiotics or Anaesthetics, and its First ESEM Characterization

5 S. Peers, P. Alcouffe, A. Montembault*, C. Ladavière*

Lyon 1 University, UMR CNRS 5223, IMP, 15 boulevard André Latarjet, 69622
Villeurbanne Cedex, France

*Corresponding authors: alexandra.clayer-montembault@univ-lyon1.fr (A. Montembault),
10 catherine.ladaviere@univ-lyon1.fr (C. Ladavière).

Abstract

This work describes the characterization of an original liposomes/hydrogel assembly, ~~as well as and~~ its application as a delayed-release system of antibiotics and anaesthetics. This system
15 corresponds to drug-loaded liposomes entrapped within a ~~three-dimensional matrix of~~ chitosan (CS) physical hydrogel. To this end, a suspension of pre-formed 1,2-dipalmitoyl-*sn*-
glycero-3-phosphocoline (~~DPPE~~) liposomes loaded with an antibiotic (rifampicin, RIF), an
anaesthetic (lidocaine, LID), or a model fluorescent molecule (carboxyfluorescein, CF), was
added to a CS solution. The CS gelation was subsequently carried out ~~according to optimized~~
20 ~~experimental conditions, and by using a reproducible process~~, without any trace of chemical
cross-linking agent or organic solvent in the final system. Liposomes within the resulting
gelled CS matrix were ~~characterized~~ for the first time by environmental scanning electron
microscopy (~~ESEM~~) ~~allowing the observation of hydrated samples maintained in their native~~
~~state. Concerning the rheological behaviour, the addition of liposomes in the CS matrix (at a~~
25 ~~lipid/CS mass ratio of 0.06 w/w) showed no significant variation on the rheological properties~~
~~of resulting assemblies (unchanging elastic and viscous moduli). Based on these evidences,~~
The release of drugs from the assembly was investigated by fluorescence or UV spectroscopy.
The cumulative release profiles of RIF and LID (and also CF for comparison) were found to
be lower from the “drug-in-liposomes-in-hydrogel” (DLH) assembly in comparison to “drug-
30 in-hydrogel” (DH) system (~~ca 11.6%, 7.5%, and 16.9%, for RIF, LID, and CF,~~
~~respectively). The concept of delayed release of several drugs with a biomedical interest for~~
~~this assembly was thus demonstrated.~~

Keywords

Chitosan, physical hydrogels, liposomes, drug delivery systems, carboxyfluorescein,
35 rifampicin, lidocaine.

1. Introduction

The property of prolonged release of therapeutic agents from liposomes or biocompatible
40 gels, and particularly **chitosan (CS)** hydrogels, has been widely investigated during the last
decade. Liposomes were the first drug delivery systems demonstrating the transition from
concept to clinical application [1]–[3], and several liposomal formulations are now
commercially available [4]. Concerning the CS hydrogels, thanks to their biocompatibility
[5], biodegradability [6] and bioactive properties (*e.g.*, mucoadhesivity [7] or bacteriostaticity
45 [8]), they are frequently considered for biomedical applications [9]. For instance, CS
hydrogels have been used as effective biomaterials for the regeneration of different tissues as
skin [10], [11], cartilage [12], [13], bone [14], muscle [15], or neural tissue [16]. They also
showed a considerable interest for the delayed release of hydrophilic and hydrophobic drugs,
growth factors, and proteins [7], [17]–[19].

50 Despite the great advantages in using liposomes in biomedical area, their main drawbacks
can be their fast elimination from the blood, the capture by the reticuloendothelial system, and
their low encapsulation efficiency [3], [20]. As regards the hydrogels, their limitation is the
initial fast, burst-like, and uncontrolled release of drugs. To overcome these disadvantages of
both drug delivery systems, liposomes, expected to act as drug reservoirs, have been added
55 into CS hydrogels. Indeed, this strategy could be interesting to maintain liposomes at the
delivery site, and to delay the release of entrapped drugs from hydrogels. This has already
been observed for the release of bromotymol blue [21], calcein [22], ofloxacin [23],
doxorubicin [24], cytarabine [25], or hormones [26] incorporated **in chitosan drug-in-
liposome-in-hydrogel (DLH)** assemblies. Nevertheless, it is worthy of note that the CS
60 hydrogels described in these studies were elaborated thanks to the addition of a cross-linking
agent in the gel formulation. However, such compounds can be cytotoxic, which significantly
diminishes the biomedical interest of the whole assembly [27]. Moreover, most of these
studies deal with antibiotics or anticancer agents, but to the best of our knowledge, none
refers to the incorporation of anaesthetics into CS DLH assemblies.

65 The work described herein follows a previous investigation already achieved in our team
on the elaboration of these DLH assemblies. **This preceding study** was about the elaboration
of DLH assemblies and their interesting property of delayed-release of a model water-soluble
molecule, **carboxyfluorescein (CF)** [28]. In this present work, one of the goals is to
70 demonstrate that this property can be transferred to molecules of biomedical interest, such as
antibiotics (RIF) and anaesthetics (LID), both **relatively** water soluble. CF is also examined as
reference, in order to compare the release of these three water-soluble molecules with
different chemical nature and molar masses. Another crucial aim of this work is to prove by
environmental scanning electron microscopy (ESEM) the presence of liposomes into the CS
hydrogel using observation conditions as close as possible to a native state. To the best of our
75 knowledge, this liposome embedment in a polymer matrix has never been observed before by
this technique.

2. Experimental part

80 *Materials*

DPPC, chloroform, acetic acid, sodium carbonate, sodium bicarbonate, ammonium
hydroxide 28%, CF (> 95% purity), RIF (> 95% purity), LID (**lidocaine hydrochloride
monohydrate**, pharmaceutical secondary standard) were purchased from Sigma Aldrich. CS
was purchased from Mahtani Chitosan Pvt. Ltd.

85

CS purification and characterization

Purification and characterization methods of CS were previously described by
Montembault *et al.* [29]. Briefly, CS was dissolved in an aqueous acetic acid solution: acid
was added to achieve the stoichiometric protonation of the polymer -NH₂ functions. The CS
90 solution was then filtered through Millipore membranes with successive pore sizes of 3.0, 1.2,
0.8, and finally 0.45 μm. The polymer was then fully precipitated by addition of dilute
ammonia (0.3 w/v). The resulting precipitate was rinsed several times with deionized water to
reach a supernatant with a neutral pH.

The weight-average molar mass of CS ($M_w = 670\,000 \pm 34\,000 \text{ g}\cdot\text{mol}^{-1}$) and dispersity
95 ($\mathcal{D} = 1.6 \pm 0.2$) were determined by size exclusion chromatography (SEC) coupled with a
differential refractometer (RI, Optilab T-rEX from Wyatt Technology), and a multi-angle
laser-light scattering detector (MALLS, HELEOS II from Wyatt Technology) equipped with a

laser operating at 664 nm. SEC was performed by means of TSKgel G2500PW and G6000PW columns. A degassed and filtered (0.1 μm) 0.15 M ammonium acetate/0.20 M acetic acid buffer (pH = 4.5) was used as eluent at a flow rate of 0.5 mL.min⁻¹. The refractive index increment (dn/dc) used for the CS analysis was 0.194 mL.g⁻¹ [30]. The degree of acetylation, DA, calculated from the ¹H NMR spectrum was close to 9.0 \pm 0.5 % [29].

Liposome elaboration and characterization

Multilamellar vesicles (MLV) and small unilamellar vesicles (SUV) were obtained by the thin film hydration method [31]. DPPC lipids were dissolved in chloroform which was then evaporated by rotary evaporation under reduced pressure until the formation of an homogeneous and thin lipid film. The latter was then hydrated by adding distilled sterile water, CF, RIF, or LID solution (see concentrations below), and stirring in a water bath at 70°C to obtain a MLV suspension. To achieve the SUV formation, the MLV suspension with a lipid concentration of 0.01 mol.L⁻¹ was then extruded 21 times through polycarbonate membrane filters with a pore size of 100 nm (Avanti Polar Lipids). The free dyes/drugs were purposely not removed from the liposomal suspension with the aim of comparing the same amounts of dyes/drugs in the both systems, DH and DLH assemblies. The optimized initial concentrations for analysis conditions of CF, RIF, and LID, were 0.1, 3.0, and 30 mmol.L⁻¹ (excepted for the release profile comparison carried out at a same concentration experiment of 3.0 mmol.L⁻¹), respectively, in a carbonate buffer (pH = 9.1, 0.1 mol.L⁻¹).

The mean hydrodynamic diameter (120 \pm 8 nm, N = 66, with N the number of measurements) and mean size distribution (polydispersity index, PDI = 0.11 \pm 0.05, N = 66) of liposome suspensions were determined in water at 25°C by dynamic light scattering (DLS) at an angle of 173°, using a Zetasizer Nano ZS (Malvern Instruments) **after a 10 times dilution of samples.**

CS physical hydrogels elaboration and liposome incorporation into CS physical hydrogels

CS physical hydrogels were prepared from aqueous CS solutions, without any organic solvent, cross-linking agent or additive, as described by Montembault *et al.* [32]. The purified CS was firstly dissolved in an aqueous acetic acidic solution in order to achieve CS solutions concentrated at 2% (w/w). The amount of acid added corresponded to the amount necessary to stoichiometrically protonate -NH₂ sites. After complete CS dissolution, 800 μL of liposome (incorporating CF, RIF, or LID) suspension, or 800 μL of CF, RIF, or LID solution (at 0.1, 3.0 or 30 mmol.L⁻¹ in a carbonate buffer pH 9.1, respectively) were added in 4.8 g of CS

solution, and the whole was stirred (magnetic stirrer, 250 rpm) for 5 min at room temperature. The solution was then transferred in a Petri dish (diameter 35 mm) and let to stand for degassing for 3 hours. The Petri dish was put in contact with gaseous ammonia to achieve gelation (practically, the dish was displayed over 100 mL of an aqueous solution of ammonia at a concentration of 2 mol.L⁻¹ in a glass reactor). The solution was let for 15h in the reactor. After taking it off from the reactor, the formed hydrogel was repeatedly washed with deionized water to eliminate the excess of ammonia and ammonium salts. The washing protocol used is described as follows: i) the gel was successively immersed into 3 mL of deionised water during 15 min for the first five washings, ii) then, during 30 min for the next 4 washings, iii) and 45 min for the following 3 washings.

Dye/drug release measurements from DH and DLH assemblies

Dye/drug release is studied during the washing protocol of DH and DLH assemblies. The gel was immersed into 3 mL of deionised water. This “washing” water was regularly removed and replaced by a fresh one. Each collected washing water was diluted in a phosphate buffer (pH = 9.1, 0.1 mol.L⁻¹), and analyzed either by fluorescence spectroscopy (for CF measurements) or by UV spectroscopy (for RIF and LID measurements) to estimate the amount of dye/drug released during this considering washing step. The time interval between two washing steps was 15 min for the first 5 ones, 30 min for the next 4 ones, and 45 min for the 3 final ones.

Fluorescent analyses for CF release measurements. Fluorescent analyses were carried out as previously described by Billard *et al.* [28] with a multi-mode Synergy Mx microplate reader (BioTek Instruments) at 25°C (excitation wavelength at 490 and emission wavelength at 518 nm). The fluorescence intensity of CF solutions prepared in carbonate buffer (pH = 9.1, 0.1 mol.L⁻¹) was measured as a function of the CF concentration, in the range from 1.10⁻¹⁰ to 1.10⁻⁶ mol.L⁻¹. The calibration curve (8 points) was obtained with a correlation coefficient (R²) above 0.9950.

UV analyses for RIF and LID release measurements. UV analyses were carried out with also a multi-mode Synergy Mx microplate reader (BioTek Instruments) at 25°C (at a wavelength of 334 and 262 nm for RIF and LID, respectively). The absorbance values of RIF and LID solutions prepared in a carbonate buffer (pH = 9.1, 0.1 mol.L⁻¹) were measured as a function of the RIF or LID concentration, in the range from 1.10⁻⁶ to 1.10⁻⁴ mol.L⁻¹ or 1.10⁻⁵ to

165 $1.5 \cdot 10^{-2} \text{ mol.L}^{-1}$, respectively. The calibration curves (7 points) were obtained with a correlation coefficient (R^2) above 0.9950.

Rheological measurements of DH and DLH assemblies

170 Dynamical rheological studies were performed at 25°C with an ARES rheometer (TA Instruments) equipped with a plate-plate tool of 25 mm diameter. The normal force sensor of the rheometer was used to measure the first contact between the hydrogel slab and the upper plate. The applied strain was chosen at 1% from the linear viscoelastic region. The elastic and viscous moduli of gels were measured from a constant strain frequency sweep over frequency ranges of 100-0.05 rad.s^{-1} .

175

Electron microscopy of DH and DLH assemblies

Transmission electron microscopy (TEM). TEM images of liposomal suspensions were acquired on a CM 120 Philips electron microscope at an accelerating voltage of 120 keV (at CTμ, Lyon 1 University, France). A droplet of the vesicle suspension (0.001 mol.L^{-1}) was deposited during 60 s on a 200 mesh carbon-coated grid (CF200-Cu, EMS, Delta Microscopies) for CF- and RIF-loaded liposomes, and on a 200 mesh Formvar® coated grid (FF200-Cu, EMS, Delta Microscopies) for LID-loaded liposomes. Then, a droplet of sodium silicotungstate (STS, 1% w/w) was added in the liposomal droplet and left for 60 s. Afterwards, the excess liquid was blotted off. The sample was then air-dried for at least 15 min before observation by TEM. The size and size distribution of liposomes from TEM images were analysed by ImageJ software 1.47v (NIH, Bethesda, MD).

Environmental scanning electron microscopy (ESEM). Liposomes and CS hydrogel pieces about 2 mm^2 were analysed using a FEI Quanta 250 environmental scanning electron microscope. Images were performed at 20 keV using a gaseous secondary electron detector. Samples were put to a Peltier stage maintained at 5°C with a partial water vapour pressure in the microscope chamber, and observed in a real time through a gradual reduction of water vapour pressure in the microscope chamber. At the beginning of observations, the chamber pressure was 5.5 Torr (at 5°C, relative humidity rate = 80%) to keep the hydrogels and the liposomes at a hydrated state, and was then slowly decreased to reveal the surface of hydrogels and liposomes to the dehydration state of the sample around 3 Torr (at 5°C, relative humidity rate = 40%). The purge of the microscope chamber was achieved at 5°C with custom pressure between 8 and 5.5 Torr to keep the sample in a hydrated state.

3. Results and discussion

200

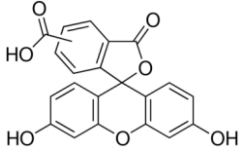
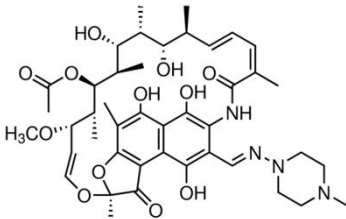
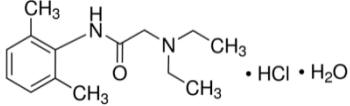
Description of molecules chosen to be incorporated in liposomes and DH assemblies

For this study, three water-soluble molecules were selected to be incorporated in liposomes, and directly in DH assemblies: RIF, LID, and CF (Table 1). RIF is one of the first choice amphiphilic anti-tuberculosis drugs. It is active against *Mycobacterium tuberculosis*,
205 *Mycobacterium leprae* and *Mycobacterium bovis* [33], [34] by forming a stable complex with DNA-dependent RNA-polymerase of bacteria, inhibiting the activity of the enzyme. RIF is thus able to kill intracellular microorganisms by entering into phagocytic cells. However, because of its poor bioavailability, efficient treatment requires a high dose of drug injected over a period a several months. This causes various serious side effects including rheumatoid,
210 allergic rashes or hepatotoxicity [35]. For these reasons, the incorporation of RIF inside liposomes is extensively studied with the goal of improving mucoadhesivity, retention time and slow release, and reducing side effects [36]–[39]. Note that its molar mass is higher than CF one (823 *versus* 376 g.mol⁻¹). LID (289 g.mol⁻¹) is a local anaesthetic agent known for its rapid action on mucosal tissues or skin for example, with a low systemic toxicity [40]. LID
215 can also be used as an antiarrhythmic agent [41]. The mechanism of action of LID is based on inhibiting nervous influx thanks to the fixation of the molecule on specific receptors of the sodium channel of nerves [42]. One of the major challenges associated to LID is the skin penetration and transdermal delivery. The insertion of LID into hydrogels [43], or in liposomes [44], [45] was consequently studied. Concerning the last molecule chosen as
220 reference, CF (376 g.mol⁻¹) is a fluorescent dye which is anionic due to its carboxylic acid group. Thanks to its water-solubility, CF is well-known as a marker of the inner cavity of liposomes [46]–[48] to examine for example the liposome/cell interactions [49], [50] or skin penetration of drugs [51].

225

230

Table 1: Structural formula and molar masses of molecules incorporated into liposomes and DH assemblies.

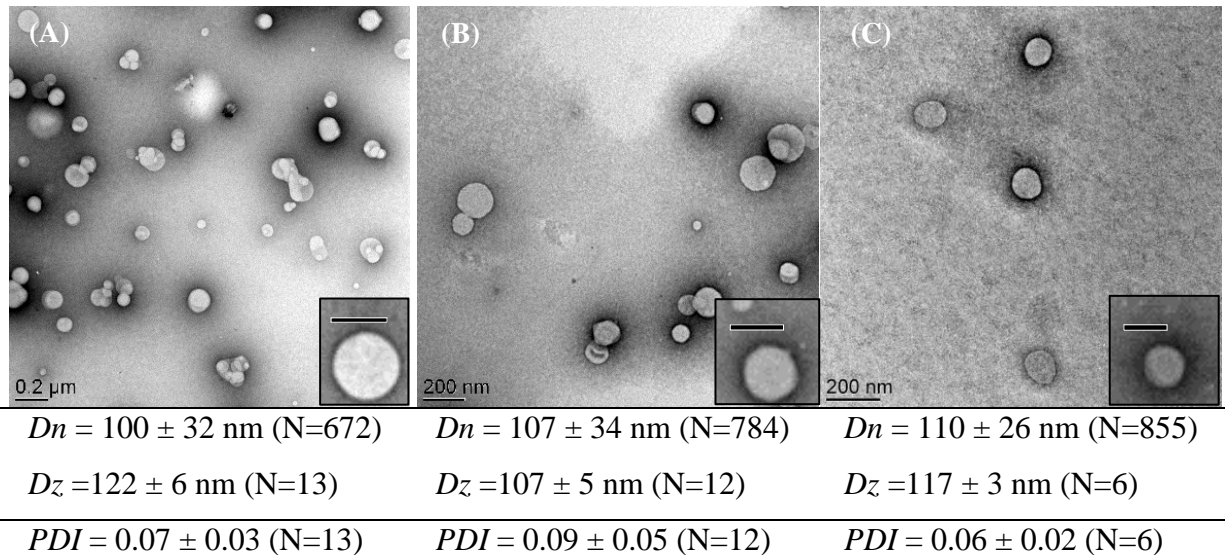
	CF	RIF	LID
Structural formula			
Molar mass (g.mol⁻¹)	376,3	822,9	288,8

235 **Elaboration and characterization of liposomes**

The first step of the elaboration of the DLH assembly is the preparation of DPPC liposomes encapsulating the drugs (RIF or LID) or dye (CF), for comparison. Liposomes were elaborated by the thin film hydration method followed by an extrusion treatment. Their characterization in terms of size and size distribution was achieved by TEM observations and

240 DLS measurements (Figure 1). TEM images reveal a satisfactory morphology with a regular round shape, regardless the entrapped molecule. Mean diameters obtained by TEM or DLS are around 120 nm (close to the pore size of 100 nm of polycarbonate membranes used for the extrusion process), and relatively low size distributions are measured (PDI *ca* 0.07). Note that

245 DLS mean diameter and size distribution of corresponding DPPC liposomes (*i.e.*, without any entrapped molecule, $D_z = 124$ nm, PDI *ca* 0.19, data not shown) are very close (confirming that the liposome size is not dependent on incorporated molecules).



250

Figure 1. TEM images (with STS contrast agent at 1% w/w) and size characterization by TEM (using Image J, mean D_n) and DLS (mean D_z , PDI) of DPPC liposomal suspensions (SUV) incorporating CF (A), RIF (B) and LID (C). N is the measurement number. The scale bars in the insets are 125 nm.

255

Elaboration of DH and DLH assemblies

After the elaboration of liposomes, the next step of DLH preparation is the mixing of dye/drug-loaded liposome suspensions with an acidic CS solution (during 5 min under stirring at room temperature). Note that for the reference DH preparation (*i.e.*, drugs directly incorporated into hydrogels, without liposome), CF, RIF or LID solutions were added instead of dye/drug-loaded liposome suspensions. The mixture was let to stand for degassing during 3 hours. Finally, the gelation of resulting mixtures was achieved according to the method described earlier [29]. This method requires no cross-linking agent or additive. The mechanism of this gelation route consists in the modification of the balance between hydrophilic and hydrophobic interactions in the system. The ammonia gas dissolved into the chitosan solution, and neutralized amine functions. The consequence was a decrease of the apparent charge density of chitosan chains, thus favouring both hydrophobic effects and hydrogen bonds. After the formation of the hydrogel, DLH or DH assemblies were then washed several times to eliminate the formed ammonium acetate, as well as the excess of ammonia.

270

Microscopy characterization of DH and DLH assemblies

275 With the aim of confirming the presence of liposomes in the hydrogels, a well-suitable microscopic technique was used. Indeed, ESEM allows the observation of specimens in their hydrated state thanks to partial vacuum inside the specimen chamber without any further sample preparation [52]. ESEM has been already used for the visualisation of liposomes [53]–[56], but DLH assemblies have never been observed by ESEM to the best of our knowledge. 280 For these observations, the incorporation of SUV-type liposomes was replaced by MLV-type ones inside hydrogels because MLV were much easier than SUV to be distinguished within the CS hydrogels. This could be explained by a better stability of MLV under electron beam (a SUV suspension was invisible in the same conditions). The SUV observation requires a higher magnification than MLV (mean diameter of MLV measured by DLS was found to be 285 between 1.5 and 2.9 μm) which implies higher electron dose rate per area destroying them (higher curvature radius). Liposomal suspensions (loaded with CF, RIF, LID, see images in SI), hydrogels with and without dye/drug-loaded MLV were observed by ESEM (Figure 2), thanks to a gradually pressure decrease in the chamber.

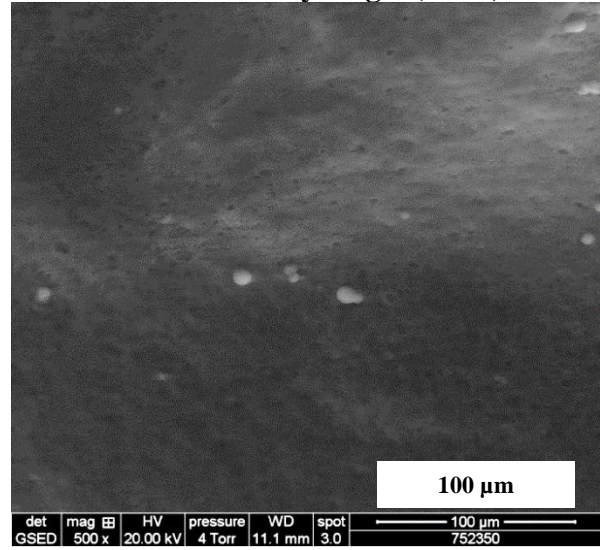
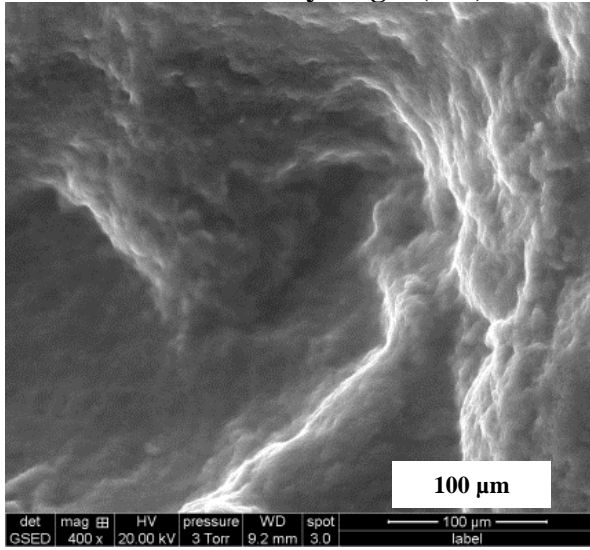
Images were obtained at 5°C with pressure around 3.5 Torr (relative humidity rate = 290 50%). Similar morphologies of liposomes were obtained with all the 3 formulations (given in SI). Sphere diameters were measured by Image J software and were about $3.9 \pm 1.3 \mu\text{m}$ (N = 203), $3.5 \pm 1.3 \mu\text{m}$ (N = 200) and $5.7 \pm 2.1 \mu\text{m}$ (N = 51) for CF, RIF, and LID liposomal suspensions, respectively. Relatively high size dispersities were obtained due to liposomal preparation method (only a film hydration, without an extrusion step). It is worthy of note that 295 the observation conditions used in this work (5°C, ca 4 Torr) are similar to the ones employed by Mohammed *et al.* [55] to detect spherical MLV-type liposomes.

The left-hand column of Figure 2 corresponds to DH (without liposome) with CF (A), RIF (B), or LID (C), and the right-hand column shows the DLH assemblies, with liposomes incorporating CF (A), RIF (B) or LID (C). These ESEM images, taken at a pressure of ca 3.5 300 Torr, reveal spheres relatively well dispersed in the CS matrix. Note that the ESEM chamber pressure has to be below 4 Torr to detect liposomes into the polymer matrix. The decrease of this pressure leads to a dehydration of CS hydrogel while liposomes remain intact (in a range of pressure ca 4 to 2.8 Torr). However, after a drastic decrease of pressure in the chamber (below 2.8 Torr), even the liposomes undergo a dehydration and lose their spherical shape. 305 This has also been observed by Mohammed *et al.* below 1.9 Torr [55].

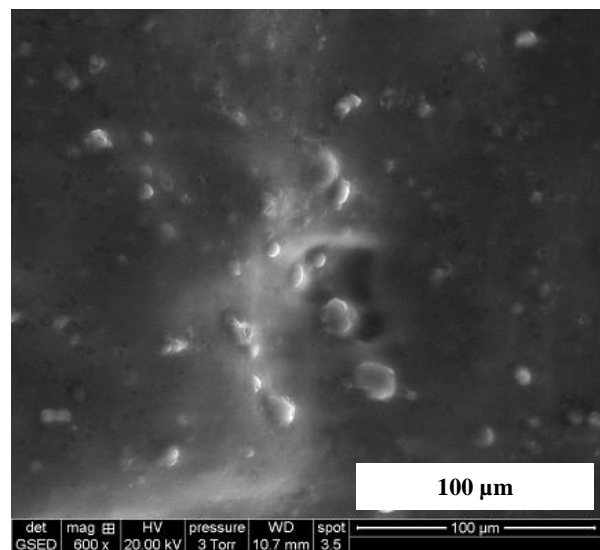
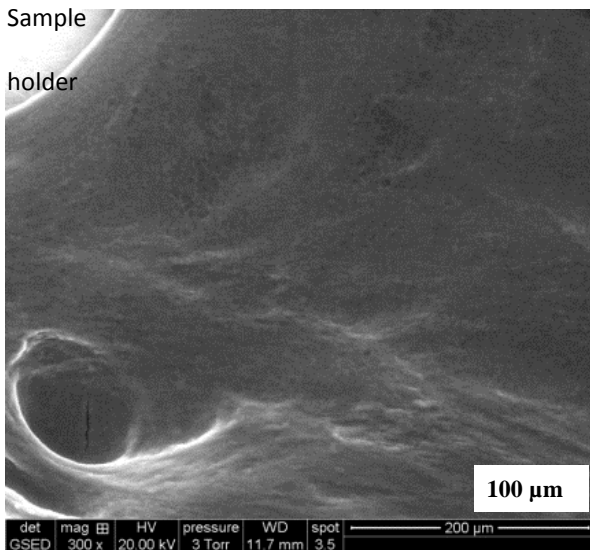
**Dye/Drug directly
inside the CS hydrogel (DH)**

**Dye/Drug-loaded MLV
inside the CS hydrogel (DLH)**

(A)



(B)



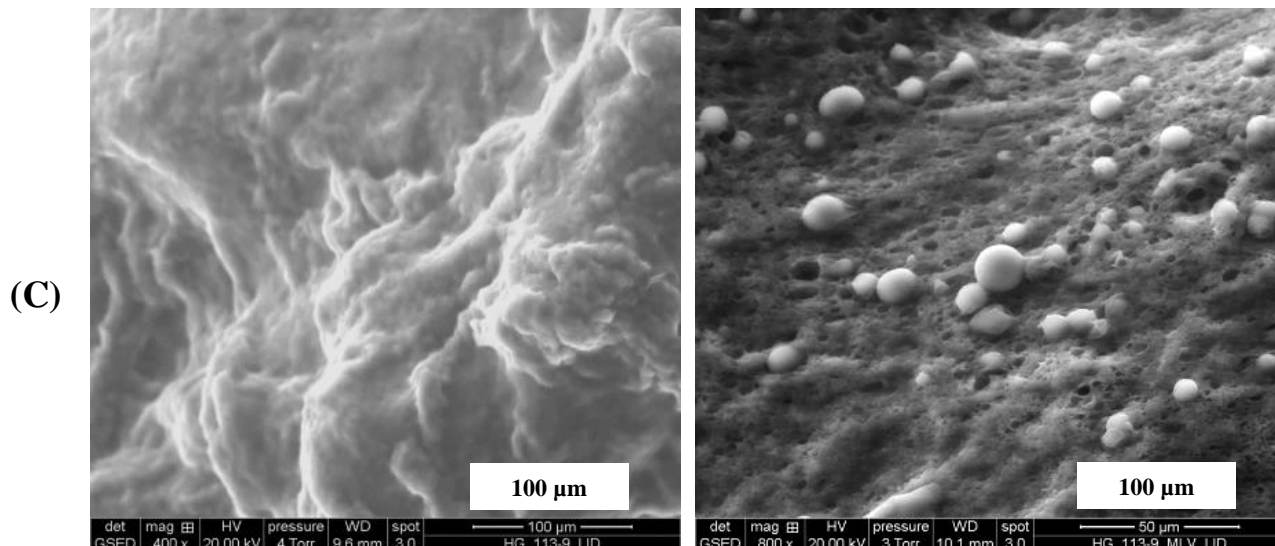


Figure 2. ESEM images at the left-hand column: DH with (A) CF, (B) RIF, (C) LID (without liposome), at the right-hand: DLH with (A) CF, (B) RIF, (C) LID MLV-loaded, at 3.5 Torr and 5°C after 12 washings ([CS] = 1.7% w/w, DA = 9%).

Size measurements of spheres observed inside hydrogels and calculated with Image J (about $6.1 \pm 3.7 \mu\text{m}$ (N = 17), $5.9 \pm 2.1 \mu\text{m}$ (N = 29) and $7.2 \pm 2.7 \mu\text{m}$ (N = 32) for CF, RIF and LID, respectively) were found to be slightly higher than liposomal suspensions ones ($3.9 \pm 1.3 \mu\text{m}$ (N = 203), $3.5 \pm 1.3 \mu\text{m}$ (N = 200) and $5.7 \pm 2.1 \mu\text{m}$ (N = 51) for CF, RIF, and LID liposomal suspensions). This difference could be explained by an easier disruption of smaller liposomes (with a higher curvature) with the decrease of chamber pressure. Indeed, this phenomenon was detected for all liposomes studied herein (example given in Figure 3).

320

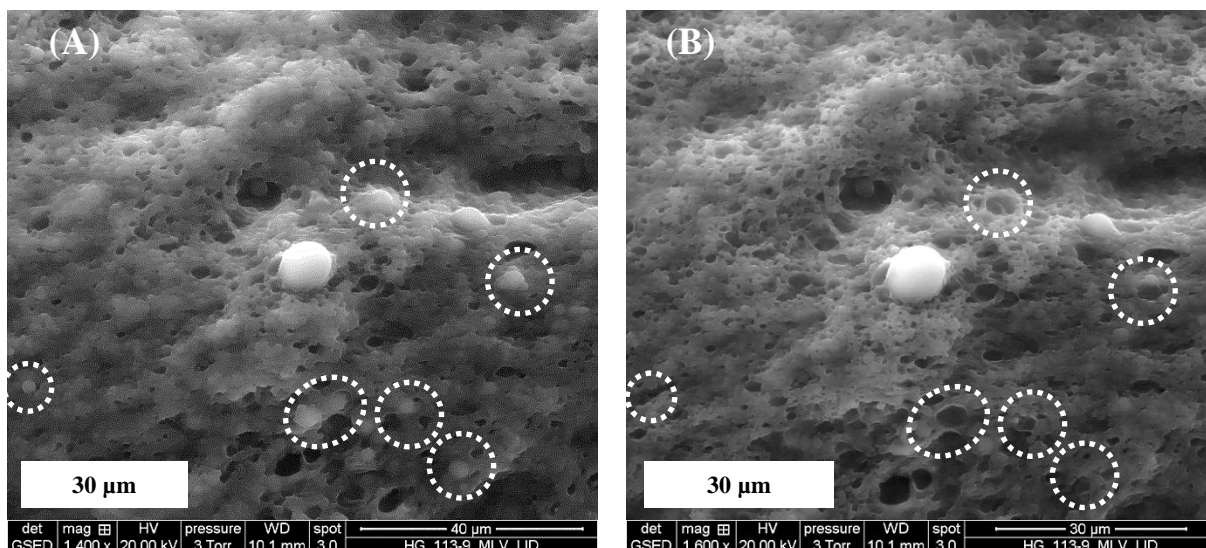


Figure 3. ESEM images of LID MLV-loaded CS hydrogels (DLH) at $t = 0$ (A) and $t =$ after 2 minutes (B) at 3.5 Torr, and 5°C, showing that the smallest liposomes with highest curvature radius disrupt the first in the ESEM chamber (a few examples are given in dotted circles as guide eyes) ([CS] = 1.7% w/w, DA = 9%).

Moreover, this difference could be also assigned to a lower number of size measurements (N) performed in the case of liposomes inside hydrogel systems (in comparison with liposomal suspensions in SI) due to the difficulty to precisely measure the size of liposomes embedded in the CS matrix (see examples of embedment in Figure 4).

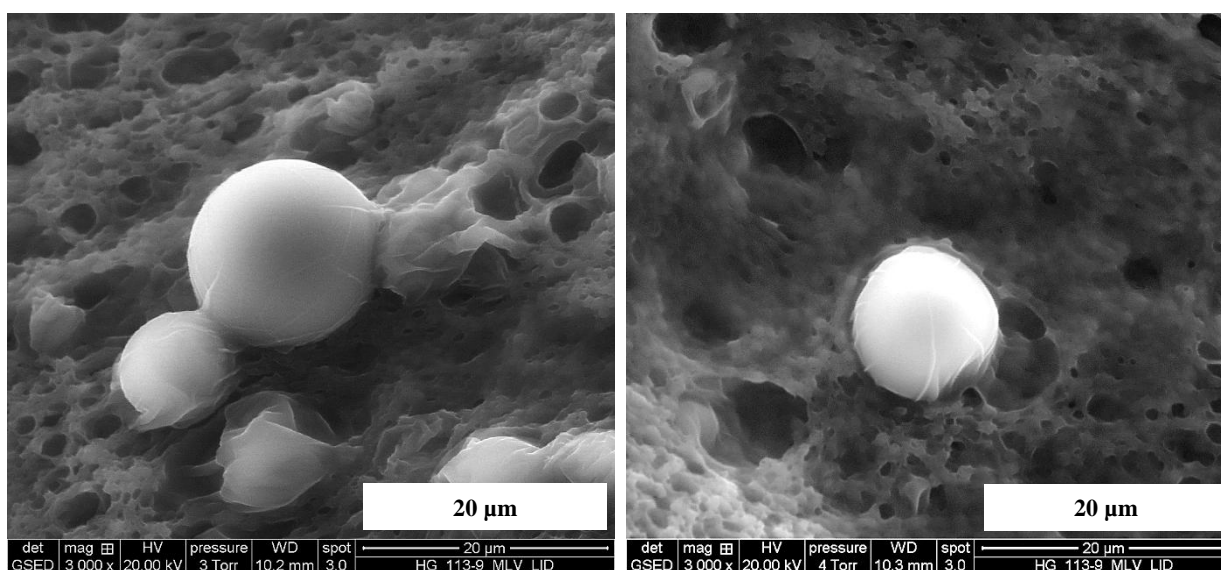


Figure 4. Examples of ESEM images at 3.5 Torr, and 5°C, showing the embedment of LID MLV-type liposomes in the CS matrix of the hydrogel (DLH).

Rheological characterization of DH and DLH assemblies

The DLH assemblies (and DH ones for comparison) were characterized by rheology measurements to determine if the presence of liposomes in the polymer solution hindered the gelation process, and interfered on the rheological behaviour of assemblies. To this end, the elastic and viscous moduli (G' and G'') were measured over a frequency-range of 100-0.05 rad.s⁻¹ (see example in SI). The average values obtained at low frequencies are presented in Figure 5 (based on the average of the 3 last measured points of the curves on the equilibrium plateau at the lowest frequencies, and then mean of minimum 3 sets of measurements).

These values named here as G'_{eq} and G''_{eq} for the DH assemblies are similar to those previously obtained by Montembault *et al.* [32]. As in previous studies [25], [28], [57], [58] about the incorporation of liposomes in CS hydrogels (with the addition of a cross-linking agent in the gel formulation), the G'_{eq} value of all DLH assemblies was found to be at least 10 times higher than G''_{eq} . All these assemblies displayed a gel-like behaviour. This proves that liposomes did not prevent the gelation of the CS solutions. Moreover, note that G'_{eq} and G''_{eq} values of DLH were close to DH. Indeed, G'_{eq} values were 500 ± 85 Pa, 450 ± 100 Pa, 420 ± 85 Pa, and 420 ± 125 Pa for the DH. G'_{eq} values were 505 ± 40 Pa, 455 ± 60 Pa, 440 ± 100 Pa, and 425 ± 50 Pa for DLH assemblies. This demonstrates that the presence of liposomes do not drastically affect the rheological properties of hydrogels (at a lipid/CS mass ratio of 0.06 w/w), regardless the molecule entrapped.

355

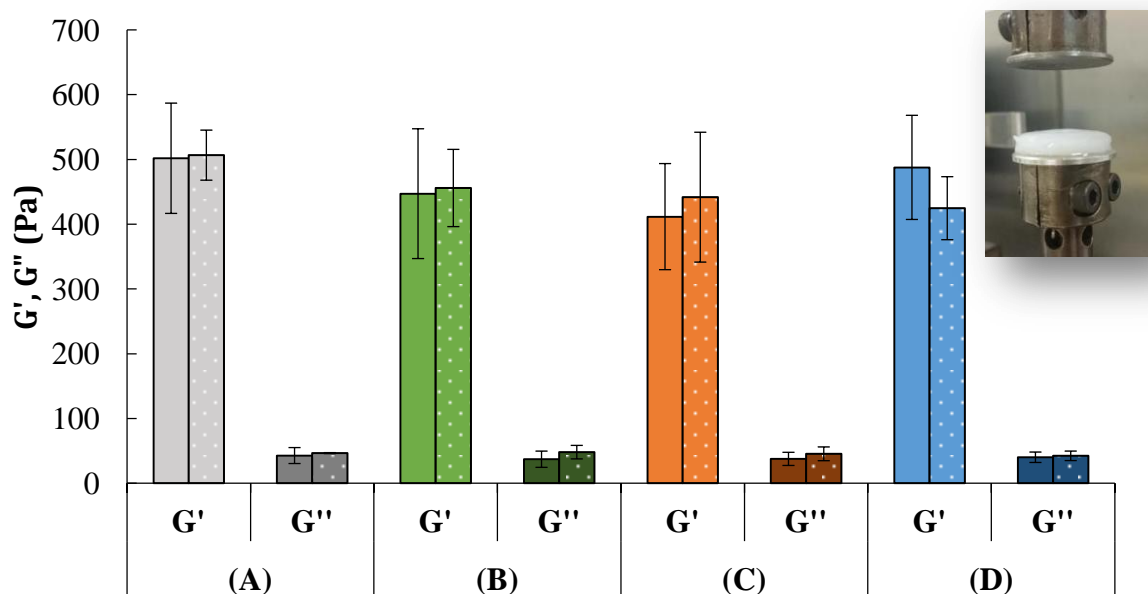


Figure 5. Variation of G'_{eq} and G''_{eq} moduli as a function of free dye/drug-loaded physical CS hydrogel (DH, filled bars) and dye/drug-loaded liposomes embedded into CS hydrogels (DLH, dotted bars) ([CS] = 1.7% w/w, DA = 9%, lipid/CS mass ratio = 0.06 w/w). (A) Reference, no dye/drug, (B) CF, (C) RIF, (D) LID. Insert corresponds to an image of a DH assembly placed between the two plates of rheometer. $N \geq 3$ for each measurement, with N the number of measurements carried out on different hydrogel batches.

The calculation of $\tan \delta$ values ($= G''_{eq} / G'_{eq}$) assesses the viscoelastic nature of materials. According to Table 2, $\tan \delta$ values were found to be very close to 0.1 for all the assemblies (DH and DLH). These values were similar to the ones obtained by Crompton *et al.* [59], and in accordance with the definition of a gel [60]. Thus, the ratio of the viscous contribution to the elastic contribution was nearly the same for all samples. This also means that these assemblies are relatively homogeneous in terms of viscoelasticity.

Table 2. $\tan \delta$ values of DH (free dye/drug loaded physical CS hydrogel) and DLH (dye/drug loaded liposomes embedded into CS hydrogels) assemblies. $N \geq 2$ for each measurement, with N the number of measurements carried out on different hydrogels batches ([CS] = 1.7% w/w).

	$\tan \delta$			
	No dye/drug	CF	RIF	LID
DH assemblies	0.085	0.082	0.092	0.082
	± 0.015	± 0.013	± 0.023	± 0.010
	(N=3)	(N=7)	(N=11)	(N=6)
DLH assemblies	0.092	0.105	0.103	0.100
	± 0.006	± 0.019	± 0.011	± 0.020
	(N=2)	(N=3)	(N=5)	(N=3)

380 Dye and drug release from DH assemblies

As a first step, dye/drug release from DH assemblies was investigated. To this end, the dye and drug molecules were directly incorporated in CS physical hydrogels, and their release

from them during the washing process was examined (Figure 6). For the sake of comparison between release profiles of dye and drugs from DH, a same dye/drug amount was inserted into CS hydrogels (*i.e.*, $2.4 \cdot 10^{-6}$ mol per hydrogel).

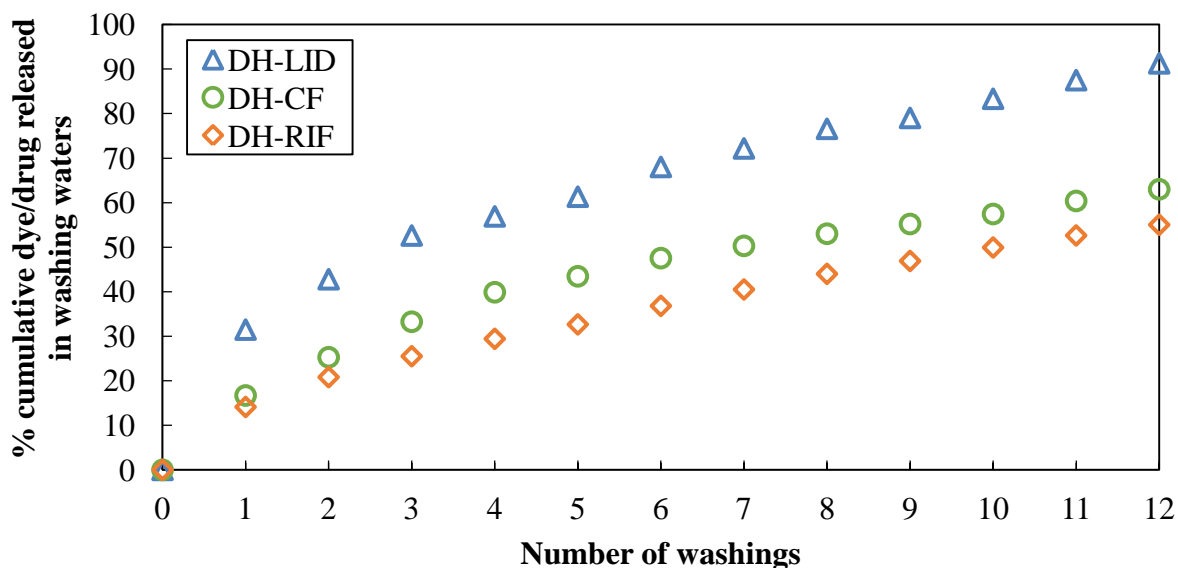


Figure 6. Dye/drug release profiles at 25°C from DH assemblies containing initially $2.4 \cdot 10^{-6}$ mol per hydrogel of RIF (N=21, orange diamonds), LID (N=3, blue triangles) and CF (N= 1, green circles).

The shape of cumulated release profiles of three water-soluble dye and drugs shows the same trend (Figure 6). Nevertheless, the release of LID molecules from DH is faster than CF molecules, which is faster than RIF molecules. The higher diffusion of CF and LID molecules through the DH assemblies could be explained by their low molar masses ($376 \text{ g} \cdot \text{mol}^{-1}$ for CF, and $289 \text{ g} \cdot \text{mol}^{-1}$ for LID), in comparison with RIF with a higher molar mass ($823 \cdot \text{mol}^{-1}$). This has been already observed in a previous study of Ruel-Gariepy *et al.* [61], which showed that the higher the molar mass, the slower the drug release with four molecules of different molar masses ($275 \text{ g} \cdot \text{mol}^{-1}$ for chlorpheniramine, $320 \text{ g} \cdot \text{mol}^{-1}$ for methylene blue, $623 \text{ g} \cdot \text{mol}^{-1}$ for calcein, and from 12,000 to 148,000 $\text{g} \cdot \text{mol}^{-1}$ for albumin). However, considering this molar mass aspect, the release of CF molecules is surprisingly slow in comparison of LID ones. This behaviour could be also assigned to electrostatic aspects. Indeed, LID are cationic molecules (tertiary amine group, $\text{pK}_a \sim 7.8$) like the CS cationic

405 chains (pKa ~ 6.5), whereas CF are anionic molecules due to their carboxylic acid group (pKa
~ 6.5). The negative charges of CF could establish attractive electrostatic interactions with
some cationic charges of CS, resulting in a slower release of CF (in comparison with anionic
LID). This has also been observed by Ruel-Gariepy *et al.* [61] who mentioned that at high
concentration, the higher the anionic charge of the molecule, the slower the release for drugs
410 loaded in CS chemical hydrogel cross-linked with glycerophosphate.

Dye and drug release from DLH assemblies, in comparison with DH

After the elaboration and characterization of DLH assemblies, the role of dye/drug
reservoirs of liposomes entrapped in CS hydrogels was examined. Consequently, dye and
415 drugs were loaded in the aqueous cavity of DPPC liposomes before to be entrapped into the
polymer network of hydrogels (DLH). Simultaneously, same dye and drugs were directly
inserted into CS hydrogels as “reference” hydrogels (DH). After CS gelation, the RIF, LID, or
CF release were studied during the washing step of hydrogels.

Before that, the stability of dye and both drugs as a function of the temperature
420 increase (performed during the liposome elaboration) and pH variations (acidic medium and
ammonia atmosphere implemented during the gelation process) was checked. All these
conditions did no lead to a shift of RIF, LID absorption peaks, and CF fluorescence emission
peak (data not shown).

Firstly, the CF release was monitored in the washing waters by fluorescence
425 measurements ($\lambda_{\text{excitation}} = 490 \text{ nm}$ and $\lambda_{\text{emission}} = 518 \text{ nm}$). Concerning RIF and LID, they were
assayed by UV spectroscopy at 334 nm for RIF) and 262 nm for LID. For this purpose,
samples of each washing water were collected and diluted into a phosphate buffer solution
(pH = 9.1, 0.1 M) before being assayed. The release of dye/drugs is then estimated thanks to a
calibration curve, established for each molecule. Experimental data were compared between
430 dye/drug encapsulated in MLV (dotted symbols) or SUV (full symbols) embedded in CS
hydrogels, and dye/drug directly loaded into polymer network (open symbols). Note that for
analytical reasons, different dye/drug concentrations were used depending on the drug
entrapped. In contrast, for both DH and DLH assemblies, the initial total dye/drug amount for
each molecule was strictly equal. Average cumulated percentages of CF, RIF and LID
435 released in each washing water are given as a function of the number of washings.

Firstly, the model CF release analysis (Figure 7) was performed in order to compare
with the previous results obtained in the team with only SUV-type liposomes [28]. Figure 7
shows the average cumulated percentage of CF released from DLH in each washing water,

with an average final cumulative release of $ca 57 \pm 4 \%$ for CF-loaded SUV (N=4), $72 \pm 5 \%$ for CF-loaded MLV (N=4), and $74 \pm 3 \%$ for CF in CS physical hydrogel (N=6). As observed by Billard *et al.* [28] in the previous study, the release of the dye is delayed when CF is incorporated in SUV before being entrapped in the CS hydrogel after the same number of washings. Thanks to the liposomes embedded into the polymer network, acting as a drug “reservoir”, and also creating a second diffusion barrier to drug diffusion, the release of CF through the DLH incorporating SUV is slower than DH.

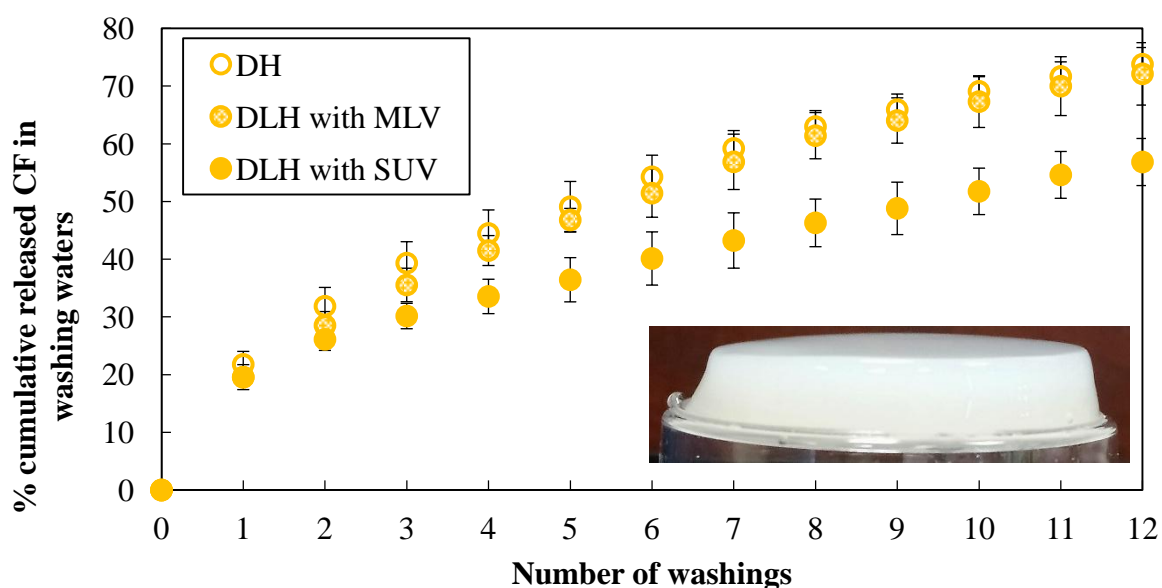
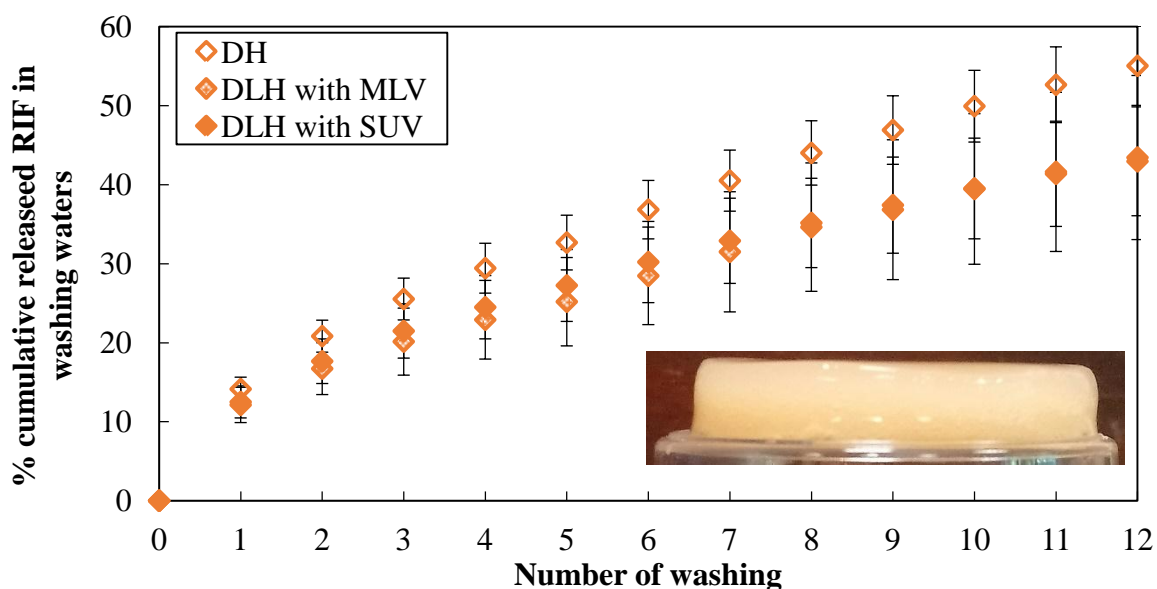


Figure 7. CF release profile at 25°C from CS hydrogels containing CF ($[CF]_i = 10^{-4} \text{ M}$, $n_{CF} = 8.10^{-8} \text{ mol}$) without liposome (empty circles, N=6) or CF loaded MLV (dotted circles, N=4) or SUV (filled circles, N=4). $[CS] = 1.7\%$, $DA = 9\%$ (w/w). Inset corresponds to a photography of a CF-DLH.

After confirming the CF delayed release from DLH, the same experiment was carried out with an antibiotic, such as RIF. Figure 8 exhibits the average cumulated percentage of RIF released from DLH in each washing water, with an average final cumulative release of $ca 43 \pm 7 \%$ for RIF-loaded SUV (N=21), $43 \pm 10 \%$, for CF-loaded MLV (N=4) and $55 \pm 5 \%$ for RIF in CS physical hydrogel (N=21). The trends for RIF loaded SUV and free RIF directly

incorporated in CS physical hydrogel are very similar to the ones obtained for CF, with a difference of more than 10% between DH and DLH.



465

Figure 8. RIF release profile at 25°C from CS hydrogels containing RIF ($[RIF]_i = 3 \cdot 10^{-3}$ M) without liposome (empty diamonds, N=21), RIF loaded MLV (dotted diamonds, N=4) or SUV (filled diamonds, N=21). [CS] = 1.7%, DA = 9% (w/w). Inset corresponds to a photograph of a RIF-DLH.

470

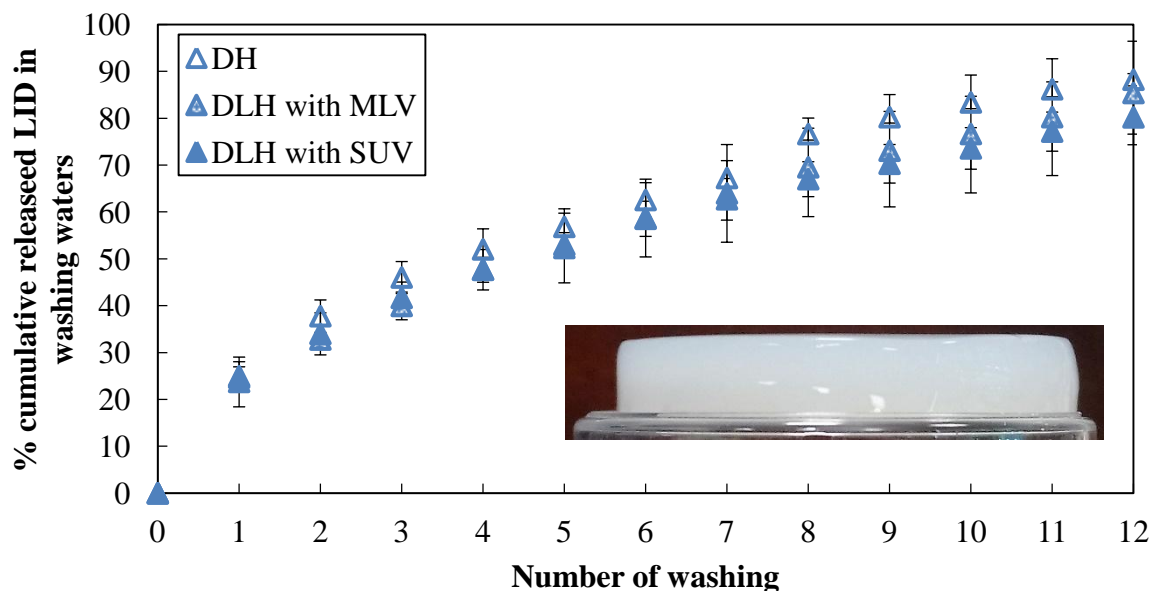
After the release analysis of an antibiotic, the release of an anaesthetic, LID, was studied. Figure 9 displays the average cumulated percentage of LID released from DLH in each washing water, with an average final cumulative release of $ca 80 \pm 4$ % for LID-loaded SUV (N=2), 85 ± 11 % for LID-loaded MLV (N=1), and 88 ± 1 % for LID in CS physical hydrogel (N=5). SUV embedded in the CS matrix act as “reservoirs” and delay the release of the LID incorporated in DLH assemblies.

475

480

The results also showed that the release profiles of DLH with molecules of interest-loaded MLV were quite similar to molecules of interest-loaded-SUV, even if the trend was less pronounced. Ciobanu *et al.* [22] observed that the release was more delayed for MLV incorporated into hydrogels (*versus* SUV). The authors explained this trend to the better drug encapsulation efficiency of MLV in comparison to SUV. On the contrary, Hurler *et al.* [62]

obtained a faster release for MLV incorporated into hydrogels, although any significant
485 difference on the release profiles of mupirocine from liposomes with various diameters was
detected.



490

Figure 9. LID release profile at 25°C from CS hydrogels containing LID ($[LID]_i = 3 \cdot 10^{-2}$ M) without liposome (N=5), LID loaded MLV (N=1) or LID loaded SUV (N=2). [CS] = 1.7%, DA = 9% (w/w). Inset corresponds to a photography of a LID-DLH.

495

4. Conclusions

In this work, biocompatible “liposomes in hydrogels” assemblies were successfully elaborated without any cross-linking agent or additive. Liposomes were able to incorporate a model water-soluble dye (carboxyfluorescein), as well as different water-soluble active agents
500 such as rifampicin or lidocaine. They were efficiently then embedded into chitosan physical hydrogels without implying the modification of their rheological properties, regardless of the dye or drug loaded. The presence of liposomes inside the polymer matrix of hydrogel was confirmed for the first time by ESEM thanks to a gradually decrease of the water vapour pressure in the microscope chamber. Measurements of dye or drug release from hydrogels
505 during the washing step showed that the loading of dye/drug in DPPC liposomes delays their escape through the system. Consequently, cumulative final release of CF, RIF and LID

revealed a difference of 16.9%, 11.6% and 7.5% between DLH and DH assemblies, respectively. This is an evidence of the delayed-release property of these designed assemblies thanks to liposomes that act as drug reservoirs. The influence of the lipid/CS mass ratio, CS acetylation degree, as well as lipid composition still need be explored for a better understanding of the release mechanism of different active agents through these systems. Furthermore, the simultaneous release of a cocktail of drugs could also be studied by incorporating two or more drugs with different biomedical properties in the same system. The *in vivo* release of drugs loaded in these “liposomes in hydrogels” assemblies is also planned to be studied. Indeed, these systems could be promising candidates in biomedical applications for example as wound dressings.

Acknowledgments

This work was financially supported by a grant from the French Ministry of Higher Education and Research. The authors gratefully acknowledge the “CTμ” (Centre Technologique des Microstructures de l’Université Lyon1) and “liquid chromatography” (Institut de Chimie de Lyon) platforms for the access to TEM, ESEM, and MALLS/RI/SEC, respectively.

References

- [1] T. M. Allen and P. R. Cullis, “Liposomal drug delivery systems: From concept to clinical applications,” *Adv. Drug Deliv. Rev.*, vol. 65, no. 1, pp. 36–48, 2013.
- [2] M. Pinheiro, M. Lucio, J. L. F. C. Lima, and S. Reis, “Liposomes as drug delivery systems for the treatment of TB,” *Nanomed.*, vol. 6, no. 8, pp. 1413–1428, 2011.
- [3] V. P. Torchilin, “Recent advances with liposomes as pharmaceutical carriers,” *Nat. Rev. Drug Discov.*, vol. 4, no. 2, pp. 145–160, 2005.
- [4] Y. (Chezy) Barenholz, “Doxil® — The first FDA-approved nano-drug: Lessons learned,” *J. Controlled Release*, vol. 160, no. 2, pp. 117–134, 2012.
- [5] H. Ueno, T. Mori, and T. Fujinaga, “Topical formulations and wound healing applications of chitosan,” *Adv. Drug Deliv. Rev.*, vol. 52, no. 2, pp. 105–115, 2001.
- [6] S. Hirano, “Bio-compatibility of chitosan by oral and intravenous administrations,” *Polym. Mater. Eng. Sci.*, vol. 59, pp. 897–901, 1988.
- [7] N. Bhattarai, J. Gunn, and M. Zhang, “Chitosan-based hydrogels for controlled, localized drug delivery,” *Adv. Drug Deliv. Rev.*, vol. 62, no. 1, pp. 83–99, 2010.
- [8] Z. Guo *et al.*, “Novel derivatives of chitosan and their antifungal activities in vitro,” *Carbohydr. Res.*, vol. 341, no. 3, pp. 351–354, 2006.
- [9] M. Dash, F. Chiellini, R. M. Ottenbrite, and E. Chiellini, “Chitosan—A versatile semi-synthetic polymer in biomedical applications,” *Prog. Polym. Sci.*, vol. 36, no. 8, pp. 981–1014, 2011.
- [10] M. P. Ribeiro *et al.*, “Development of a new chitosan hydrogel for wound dressing,” *Wound Repair Regen.*, vol. 17, no. 6, pp. 817–824, 2009.
- [11] N. Boucard *et al.*, “The use of physical hydrogels of chitosan for skin regeneration following third-degree burns,” *Biomaterials*, vol. 28, no. 24, pp. 3478–3488, 2007.

- 550 [12] J.-K. Francis Suh and H. W. T. Matthew, "Application of chitosan-based polysaccharide biomaterials in cartilage tissue engineering: a review," *Biomaterials*, vol. 21, no. 24, pp. 2589–2598, 2000.
- [13] A. Montembault, K. Tahiri, C. Korwin-Zmijowska, X. Chevalier, M.-T. Corvol, and A. Domard, "A material decoy of biological media based on chitosan physical hydrogels: application to cartilage tissue engineering," *Biochimie*, vol. 88, no. 5, pp. 551–564, 2006.
- 555 [14] B. Sun *et al.*, "The osteogenic differentiation of dog bone marrow mesenchymal stem cells in a thermo-sensitive injectable chitosan/collagen/ β -glycerophosphate hydrogel: in vitro and in vivo," *J. Mater. Sci. Mater. Med.*, vol. 22, no. 9, pp. 2111–2118, 2011.
- [15] S. M. Maryam Hajiabbas, "Chitosan-gelatin sheets as scaffolds for muscle tissue engineering," *Artif. Cells Nanomedicine Biotechnol. Print*, vol. 43, no. 2, 2013.
- 560 [16] J. Chedly *et al.*, "Physical chitosan microhydrogels as scaffolds for spinal cord injury restoration and axon regeneration," *Biomaterials*, vol. 138, pp. 91–107, 2017.
- [17] E. P. D. Azevedo, "Chitosan hydrogels for drug delivery and tissue engineering applications," *Int. J. Pharm. Pharm. Sci.*, vol. 7, no. 12, pp. 8–14, 2015.
- [18] L. Liu, Q. Gao, X. Lu, and H. Zhou, "In situ forming hydrogels based on chitosan for drug delivery and tissue regeneration," *Asian J. Pharm. Sci.*, 2016.
- 565 [19] S. M. Ahsan, M. Thomas, K. K. Reddy, S. G. Sooraparaju, A. Asthana, and I. Bhatnagar, "Chitosan as biomaterial in drug delivery and tissue engineering," *Int. J. Biol. Macromol.*, vol. 110, pp. 97–109, 2018.
- [20] D. Sharma, A. a. E. Ali, and L. R. Trivedi, "An Updated Review on: Liposomes as drug delivery system," *PharmaTutor*, vol. 6, no. 2, pp. 50–62, 2018.
- 570 [21] K. P. Rao and S. Alamelu, "Effect of crosslinking agent on the release of an aqueous marker from liposomes sequestered in collagen and chitosan gels," *J. Membr. Sci.*, vol. 71, no. 1, pp. 161–167, 1992.
- [22] B. C. Ciobanu, A. N. Cadinoiu, M. Popa, J. Desbrières, and C. A. Peptu, "Modulated release from liposomes entrapped in chitosan/gelatin hydrogels," *Mater. Sci. Eng. C*, vol. 43, pp. 383–391, 2014.
- 575 [23] K. M. Hosny, "Preparation and Evaluation of Thermosensitive Liposomal Hydrogel for Enhanced Transcorneal Permeation of Ofloxacin," *AAPS PharmSciTech*, vol. 10, no. 4, pp. 1336–1342, 2009.
- 580 [24] López- Noriega Adolfo *et al.*, "Hyperthermia- Induced Drug Delivery from Thermosensitive Liposomes Encapsulated in an Injectable Hydrogel for Local Chemotherapy," *Adv. Healthc. Mater.*, vol. 3, no. 6, pp. 854–859, 2014.
- [25] R. Mulik, V. Kulkarni, and R. S. R. Murthy, "Chitosan-Based Thermosensitive Hydrogel Containing Liposomes for Sustained Delivery of Cytarabine," *Drug Dev. Ind. Pharm.*, vol. 35, no. 1, pp. 49–56, 2009.
- 585 [26] A. Alinaghi, M. R. Rouini, F. J. Daha, and H. R. Moghimi, "Hydrogel-embedded vesicles, as a novel approach for prolonged release and delivery of liposome, in vitro and in vivo," *J. Liposome Res.*, vol. 23, no. 3, pp. 235–243, 2013.
- [27] S.-C. Chen, Y.-C. Wu, F.-L. Mi, Y.-H. Lin, L.-C. Yu, and H.-W. Sung, "A novel pH-sensitive hydrogel composed of N,O-carboxymethyl chitosan and alginate cross-linked by genipin for protein drug delivery," *J. Controlled Release*, vol. 96, no. 2, pp. 285–300, 2004.
- 590 [28] A. Billard, L. Pourchet, S. Malaise, P. Alcouffe, A. Montembault, and C. Ladavière, "Liposome-loaded chitosan physical hydrogel: Toward a promising delayed-release biosystem," *Carbohydr. Polym.*, vol. 115, pp. 651–657, 2015.
- 595 [29] A. Montembault, C. Viton, and A. Domard, "Physico-chemical studies of the gelation of chitosan in a hydroalcoholic medium," *Biomaterials*, vol. 26, no. 8, pp. 933–943, 2005.
- [30] C. Schatz, C. Viton, T. Delair, C. Pichot, and A. Domard, "Typical Physicochemical Behaviors of Chitosan in Aqueous Solution," *Biomacromolecules*, vol. 4, no. 3, pp. 641–648, 2003.
- [31] A. D. Bangham, M. M. Standish, and J. C. Watkins, "Diffusion of univalent ions across the lamellae of swollen phospholipids," *J. Mol. Biol.*, vol. 13, no. 1, pp. 238–252, 1965.
- 600 [32] A. Montembault, C. Viton, and A. Domard, "Rheometric Study of the Gelation of Chitosan in Aqueous Solution without Cross-Linking Agent," *Biomacromolecules*, vol. 6, no. 2, pp. 653–662, 2005.

- 605 [33] "VIDAL - Rifampicine." [Online]. Available: <https://www.vidal.fr/substances/3060/rifampicine/>. [Accessed: 15-2018].
- [34] "Rifampin FDA Label - Capsule, injection (powder, lyophilized, for solution)," *AIDSinfo*. [Online]. Available: <https://aidsinfo.nih.gov/drugs/109/rifampin/63/professional>. [Accessed: 15-2018].
- 610 [35] D. J. Girling, "The hepatic toxicity of antituberculosis regimens containing isoniazid, rifampicin and pyrazinamide," *Tubercle*, vol. 59, no. 1, pp. 13–32, 1977.
- [36] N. Changsan, H.-K. Chan, F. Separovic, and T. Srichana, "Physicochemical characterization and stability of rifampicin liposome dry powder formulations for inhalation," *J. Pharm. Sci.*, vol. 98, no. 2, pp. 628–639, 2009.
- 615 [37] M. Zaru, S. Mourtas, P. Klepetsanis, A. M. Fadda, and S. G. Antimisiaris, "Liposomes for drug delivery to the lungs by nebulization," *Eur. J. Pharm. Biopharm.*, vol. 67, no. 3, pp. 655–666, 2007.
- [38] M. Zaru, M.-L. Manca, A. M. Fadda, and S. G. Antimisiaris, "Chitosan-coated liposomes for delivery to lungs by nebulisation," *Colloids Surf. B Biointerfaces*, vol. 71, no. 1, pp. 88–95, 2009.
- 620 [39] A. Gürsoy, E. Kut, and S. Özkırmılı, "Co-encapsulation of isoniazid and rifampicin in liposomes and characterization of liposomes by derivative spectroscopy," *Int. J. Pharm.*, vol. 271, no. 1–2, pp. 115–123, 2004.
- [40] Y. Wang *et al.*, "Preparation and evaluation of lidocaine hydrochloride-loaded TAT-conjugated polymeric liposomes for transdermal delivery," *Int. J. Pharm.*, vol. 441, no. 1–2, pp. 748–756, 625 2013.
- [41] D. C. Harrison, J. H. Sprouse, A. G. Morrow, and H. E. Hoff, "The antiarrhythmic properties of lidocaine and procaine amide: clinical and physiologic studies of their cardiovascular effects in man," *Circulation*, vol. 28, no. 2, pp. 486–491, 1963.
- 630 [42] "VIDAL - Lidocaïne." [Online]. Available: <https://www.vidal.fr/substances/2097/lidocaine/>. [Accessed: 15-2018].
- [43] D.-Z. Liu, M.-T. Sheu, C.-H. Chen, Y.-R. Yang, and H.-O. Ho, "Release characteristics of lidocaine from local implant of polyanionic and polycationic hydrogels," *J. Controlled Release*, vol. 118, no. 3, pp. 333–339, 2007.
- 635 [44] S.-M. Hou and H.-Y. Yu, "Comparison of absorption of aqueous lidocaine and liposome lidocaine following topical application on rabbit vessels," *J. Orthop. Res.*, vol. 12, no. 2, pp. 294–297, 1994.
- [45] M. L. González-Rodríguez, L. B. Barros, J. Palma, P. L. González-Rodríguez, and A. M. Rabasco, "Application of statistical experimental design to study the formulation variables influencing the coating process of lidocaine liposomes," *Int. J. Pharm.*, vol. 337, no. 1–2, pp. 640 336–345, 2007.
- [46] D. A. Kendall and R. C. MacDonald, "A fluorescence assay to monitor vesicle fusion and lysis," *J. Biol. Chem.*, vol. 257, no. 23, pp. 13892–13895, 1982.
- [47] J. Barbet, P. Machy, A. Truneh, and L. D. Leserman, "Weak acid-induced release of liposome-encapsulated carboxyfluorescein," *Biochim. Biophys. Acta BBA-Biomembr.*, vol. 772, no. 3, pp. 645 347–356, 1984.
- [48] J. Nishijo, S. Shiota, K. Mazima, Y. Inoue, H. Mizuno, and J. Yoshida, "Interactions of Cyclodextrins with Dipalmitoyl, Distearoyl, and Dimyristoyl Phosphatidyl Choline Liposomes. A Study by Leakage of Carboxyfluorescein in Inner Aqueous Phase of Unilamellar Liposomes," *Chem. Pharm. Bull. (Tokyo)*, vol. 48, no. 1, pp. 48–52, 2000.
- 650 [49] J. N. Weinstein, S. Yoshikami, P. Henkart, R. Blumenthal, and W. A. Hagins, "Liposome-cell interaction: transfer and intracellular release of a trapped fluorescent marker," *Science*, vol. 195, no. 4277, pp. 489–492, 1977.
- [50] E. Ralston, L. M. Hjelmeland, R. D. Klausner, J. N. Weinstein, and R. Blumenthal, "Carboxyfluorescein as a probe for liposome-cell interactions effect of impurities, and purification of the dye," *Biochim. Biophys. Acta BBA-Biomembr.*, vol. 649, no. 1, pp. 133–137, 655 1981.
- [51] D. D. Verma, S. Verma, G. Blume, and A. Fahr, "Liposomes increase skin penetration of entrapped and non-entrapped hydrophilic substances into human skin: a skin penetration and

- confocal laser scanning microscopy study,” *Eur. J. Pharm. Biopharm.*, vol. 55, no. 3, pp. 271–277, 2003.
- 660 [52] Y. Perrie, H. Ali, D. J. Kirby, A. U. R. Mohammed, S. E. McNeil, and A. Vangala, “Environmental Scanning Electron Microscope Imaging of Vesicle Systems,” in *Liposomes: Methods and Protocols*, G. G. M. D’Souza, Ed. New York, NY: Springer New York, 2017, pp. 131–143.
- 665 [53] B. Ruozi *et al.*, “AFM, ESEM, TEM, and CLSM in liposomal characterization: a comparative study,” *Int. J. Nanomedicine*, vol. 6, pp. 557–563, 2011.
- [54] Y. Perrie, A. U. R. Mohammed, A. Vangala, and S. E. McNeil, “Environmental Scanning Electron Microscopy Offers Real-Time Morphological Analysis of Liposomes and Niosomes,” *J. Liposome Res.*, vol. 17, no. 1, pp. 27–37, 2007.
- 670 [55] A. R. Mohammed, N. Weston, A. G. A. Coombes, M. Fitzgerald, and Y. Perrie, “Liposome formulation of poorly water soluble drugs: optimisation of drug loading and ESEM analysis of stability,” *Int. J. Pharm.*, vol. 285, no. 1, pp. 23–34, 2004.
- [56] S. Bibi *et al.*, “Microscopy imaging of liposomes: From coverslips to environmental SEM,” *Int. J. Pharm.*, vol. 417, no. 1, pp. 138–150, 2011.
- 675 [57] S. Mourtas, S. Fotopoulou, S. Duraj, V. Sfika, C. Tsakiroglou, and S. G. Antimisiaris, “Liposomal drugs dispersed in hydrogels: Effect of liposome, drug and gel properties on drug release kinetics,” *Colloids Surf. B Biointerfaces*, vol. 55, no. 2, pp. 212–221, 2007.
- [58] E. Ruel-Gariépy, G. Leclair, P. Hildgen, A. Gupta, and J.-C. Leroux, “Thermosensitive chitosan-based hydrogel containing liposomes for the delivery of hydrophilic molecules,” *J. Controlled Release*, vol. 82, no. 2–3, pp. 373–383, 2002.
- 680 [59] K. E. Crompton *et al.*, “Morphology and gelation of thermosensitive chitosan hydrogels,” *Biophys. Chem.*, vol. 117, no. 1, pp. 47–53, 2005.
- [60] K. Almdal, J. Dyre, S. Hvidt, and O. Kramer, “Towards a phenomenological definition of the term ‘gel,’” *Polym. Gels Netw.*, vol. 1, no. 1, pp. 5–17, 1993.
- 685 [61] E. Ruel-Gariépy, A. Chenite, C. Chaput, S. Guirguis, and J.-C. Leroux, “Characterization of thermosensitive chitosan gels for the sustained delivery of drugs,” *Int. J. Pharm.*, vol. 203, no. 1–2, pp. 89–98, 2000.
- [62] J. Hurler, O. A. Berg, M. Skar, A. H. Conradi, P. J. Johnsen, and N. Škalko-Basnet, “Improved Burns Therapy: Liposomes- in- Hydrogel Delivery System for Mupirocin,” *J. Pharm. Sci.*, vol. 101, no. 10, pp. 3906–3915, 2012.
- 690

Supporting Information

695

Embedment of Liposomes into Chitosan Physical Hydrogel for the Delayed Release of Antibiotics or Anaesthetics, and its First ESEM Characterization

700 S. Peers, P. Alcouffe, A. Montembault*, C. Ladavière*

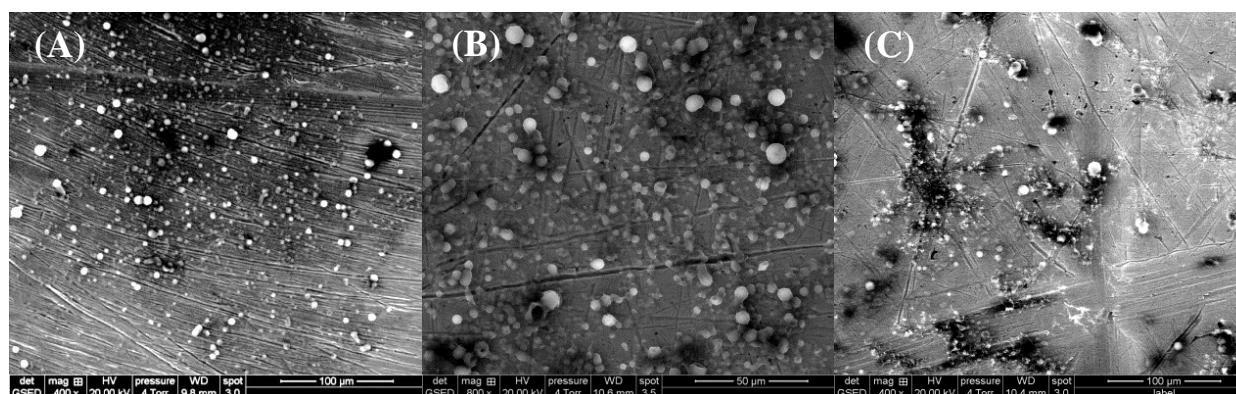
Lyon 1 University, UMR CNRS 5223, IMP, 15 boulevard André Latarjet, 69622 Villeurbanne Cedex, France

*Corresponding authors: alexandra.clayer-montembault@univ-lyon1.fr (A. Montembault),

705 catherine.ladaviere@univ-lyon1.fr (C. Ladavière).

SI. ESEM images of dye/drug-loaded MLV suspensions (0.01 mol.L^{-1}) incorporating CF (A), RIF (B), LID(C), at 4 Torr and 5°C , and size characterization by ESEM (using Image J, D_n) and DLS (D_z , PDI). N is the measurement number.

710



$D_n = 3917 \pm 1341 \text{ nm}$

(N=203)

$D_z = 2375 \pm 716 \text{ nm}$ (N=11)

$PDI = 0.44 \pm 0.29$ (N=11)

$D_n = 3484 \pm 1301 \text{ nm}$

(N=200)

$D_z = 1687 \pm 668 \text{ nm}$ (N=9)

$PDI = 0.55 \pm 0.34$ (N=9)

$D_n = 5673 \pm 2130 \text{ nm}$

(N=51)

$D_z = 2896 \pm 957 \text{ nm}$ (N=3)

$PDI = 0.47 \pm 0.12$ (N=3)

Captions of Tables and Figures

715 **Table 1.** Structural formula and molar masses of molecules incorporated into liposomes and
CS hydrogels in this work.

Table 2. Tan δ values of DH (free dye/drug loaded physical CS hydrogel) and DLH (dye/drug
loaded liposomes embedded into CS hydrogels) assemblies. $N \geq 2$ for each measurement, with
720 N the number of measurements carried out on different hydrogels batches ($[CS] = 1.7\%$ w/w).

Figure 1. TEM images (with STS contrast agent at 1% w/w) and size characterization by
TEM (using Image J, mean D_n) and DLS (mean D_z , PDI) of DPPC liposomal suspensions
(SUV) incorporating CF (A), RIF (B) and LID (C). N is the measurement number. The scale
725 bares in the insets are 125 nm.

Figure 2. ESEM images at the left-hand column: DH with (A) CF, (B) RIF, (C) LID (without
liposome), at the right-hand: DLH with (A) CF, (B) RIF, (C) LID MLV-loaded, at 3.5 Torr
and 5°C after 12 washings ($[CS] = 1.7\%$ w/w, DA = 9%).

730 **Figure 3.** ESEM images of LID MLV-loaded CS hydrogels (DLH) at $t = 0$ (A) and $t =$ after 2
minutes (B) at 3.5 Torr, and 5°C, showing that the smallest liposomes with highest curvatures
disrupt the first in the ESEM chamber (a few examples are given in dotted circles as guide
eyes) ($[CS] = 1.7\%$ w/w, DA = 9%).

735 **Figure 4.** Examples of ESEM images at 3.5 Torr, and 5°C, showing the embedment of LID
MLV-type liposomes in the CS matrix of the hydrogel (DLH).

Figure 5. Variation of G'_{eq} and G''_{eq} moduli as a function of free dye/drug-loaded physical
740 CS hydrogel (DH, filled bars) and dye/drug-loaded liposomes embedded into CS hydrogels
(DLH, dotted bars) ($[CS] = 1.7\%$ w/w, DA = 9%, lipid/CS mass ratio = 0.06 w/w). (A)
Reference, no dye/drug, (B) CF, (C) RIF, (D) LID. Insert corresponds to an image of a DH
assembly placed between the two plates of rheometer. $N \geq 3$ for each measurement, with N the
number of measurements carried out on different hydrogel batches.

745

Figure 6. Dye/drug release profiles from DH assemblies containing initially $2.4 \cdot 10^{-6}$ mol per hydrogel of RIF (N=21, orange diamonds), LID (N=3, blue triangles) and CF (N= 1, green circles).

750 **Figure 7.** CF release profile from CS hydrogels containing CF ($[CF]_i = 10^{-4}$ M) without liposome (empty circles, N=6) or CF loaded MLV (dotted circles, N=4) or SUV (filled circles, N=4). $[CS] = 1.7\%$, $DA = 9\%$ (w/w). Inset corresponds to a photography of a CF-DLH.

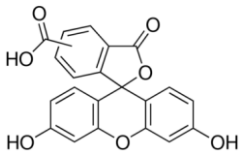
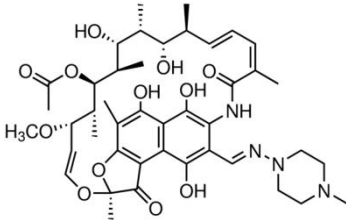
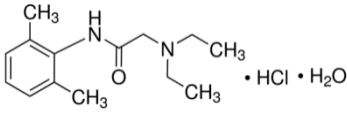
755 **Figure 8.** RIF release profile from CS hydrogels containing RIF ($[RIF]_i = 3 \cdot 10^{-3}$ M) without liposome (empty diamonds, N=21), RIF loaded MLV (dotted diamonds, N=4) or SUV (filled diamonds, N=21). $[CS] = 1.7\%$, $DA = 9\%$ (w/w). Inset corresponds to a photography of a RIF-DLH.

760 **Figure 9.** LID release profile from CS hydrogels containing LID ($[LID]_i = 3 \cdot 10^{-2}$ M) without liposome (N=5), LID loaded MLV (N=1) or SUV (N=2). $[CS] = 1.7\%$, $DA = 9\%$ (w/w). Inset corresponds to a photography of a LID-DLH.

Tables and Figures

765

770 **Table 1:** Structural formula and molar masses of molecules incorporated into liposomes and DH assemblies.

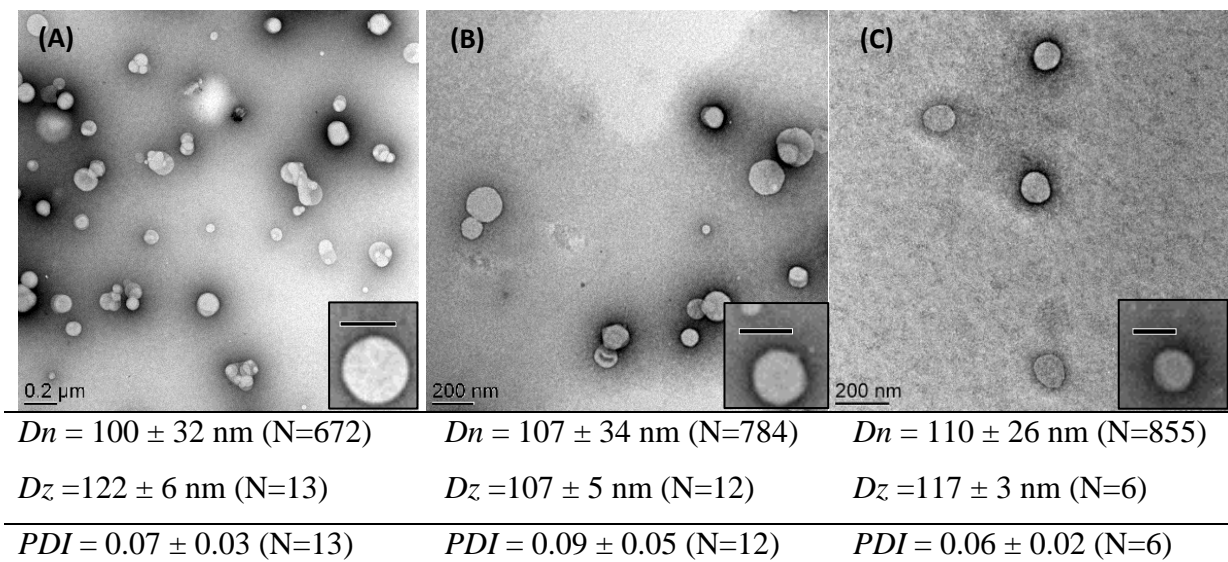
	CF	RIF	LID
Structural formula			
Molar mass (g.mol⁻¹)	376,3	822,9	288,8

775

Table 2. Tan δ values of DH (free dye/drug loaded physical CS hydrogel) and DLH (dye/drug loaded liposomes embedded into CS hydrogels) assemblies. $N \geq 2$ for each measurement, with N the number of measurements carried out on different hydrogels batches ([CS] = 1.7% w/w).

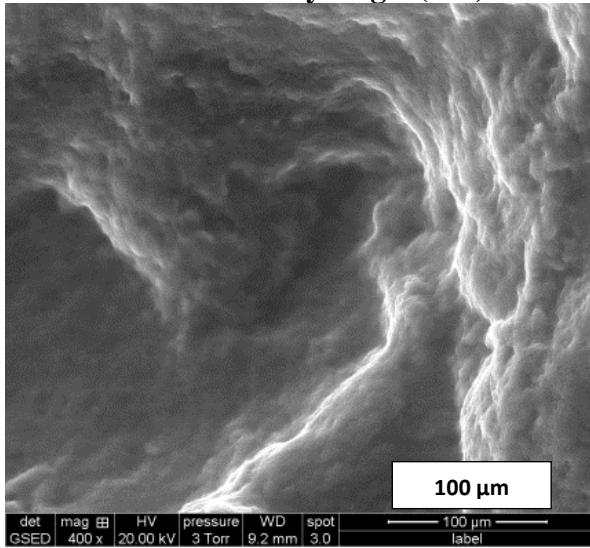
	tan δ			
	No dye/drug	CF	RIF	LID
DH assemblies	0.085	0.082	0.092	0.082
	± 0.015	$\pm 0,013$	$\pm 0,023$	± 0.010
	(N=3)	(N=7)	(N=11)	(N=6)
DLH assemblies	0.092	0.105	0.103	0.100
	± 0.006	± 0.019	± 0.011	± 0.020
	(N=2)	(N=3)	(N=5)	(N=3)

780

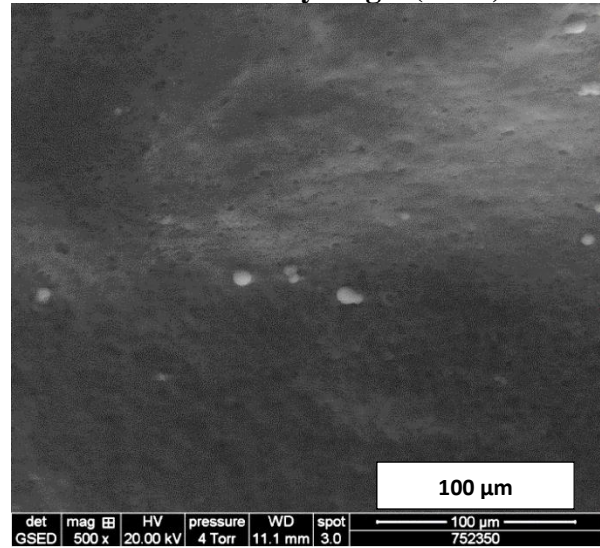


790 **Figure 1.** TEM images (with STS contrast agent at 1% w/w) and size characterization by TEM (using Image J, mean D_n) and DLS (mean D_z , PDI) of DPPC liposomal suspensions (SUV) incorporating CF (A), RIF (B) and LID (C). N is the measurement number. The scale bare in the insets are 125 nm.

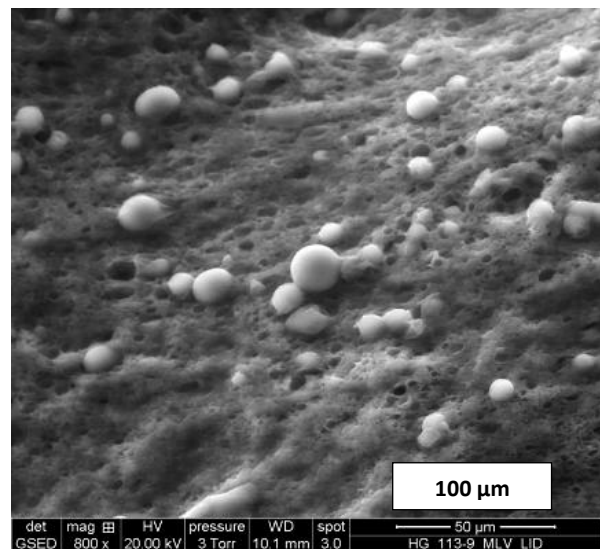
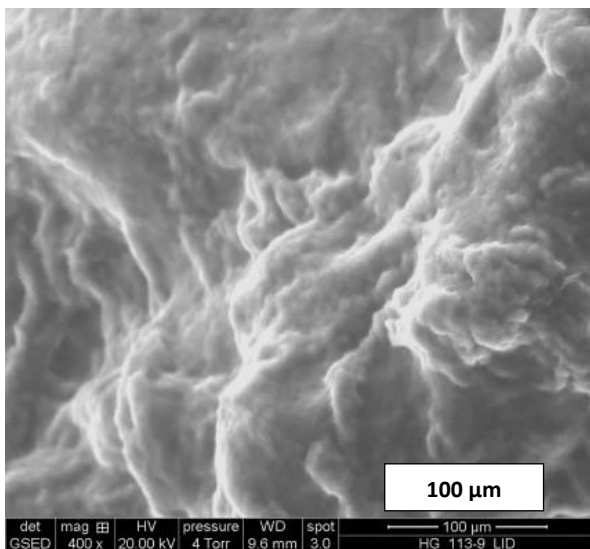
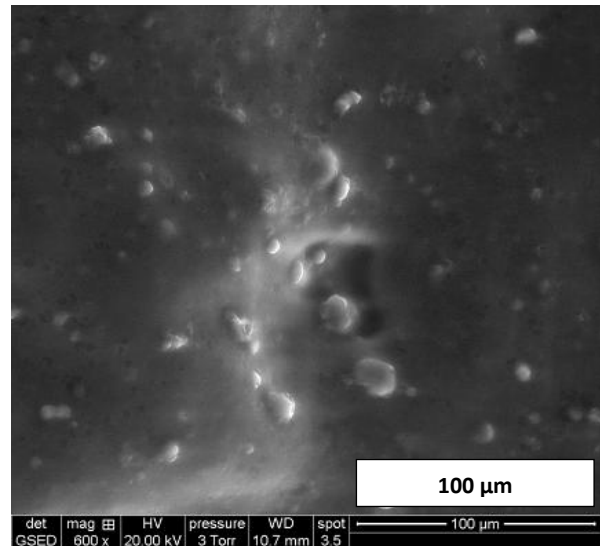
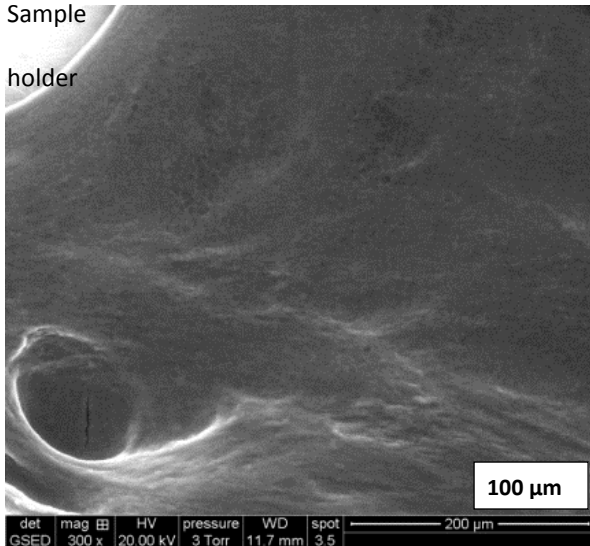
**Dye/Drugs directly
inside the CS hydrogel (DH)**



**Dye/Drug-loaded MLV
inside the CS hydrogel (DLH)**



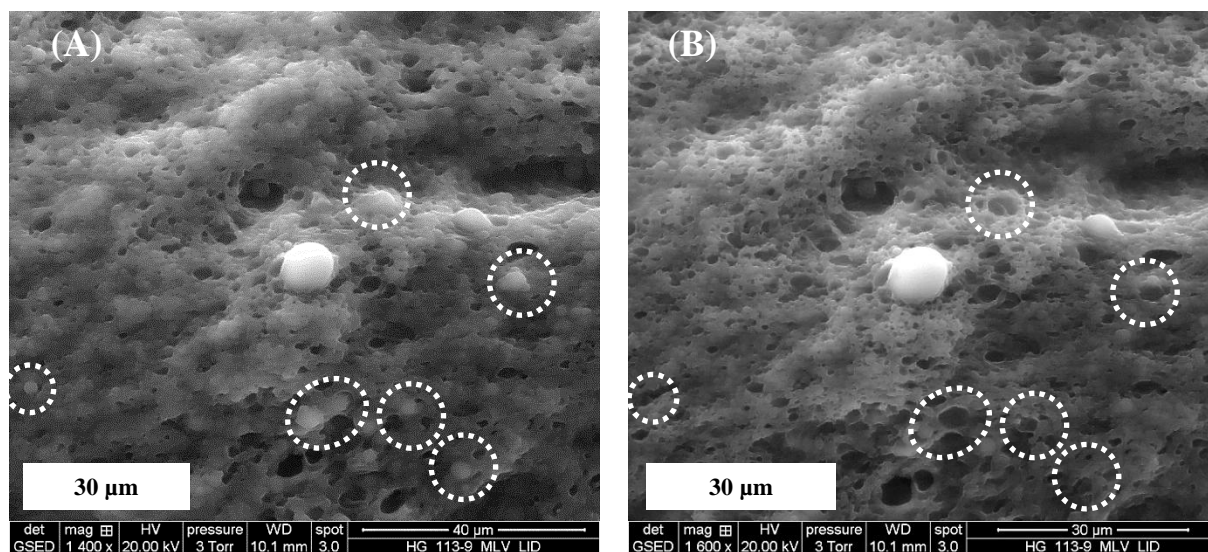
Sample
holder



795 **Figure 2.** ESEM images at the left-hand column: DH with (A) CF, (B) RIF, (C) LID (without liposome), at the right-hand: DLH with (A) CF, (B) RIF, (C) LID/MLV-loaded, at 3.5 Torr and 5°C after 12 washings ([CS] = 1.7% w/w, DA = 9%).

800

805

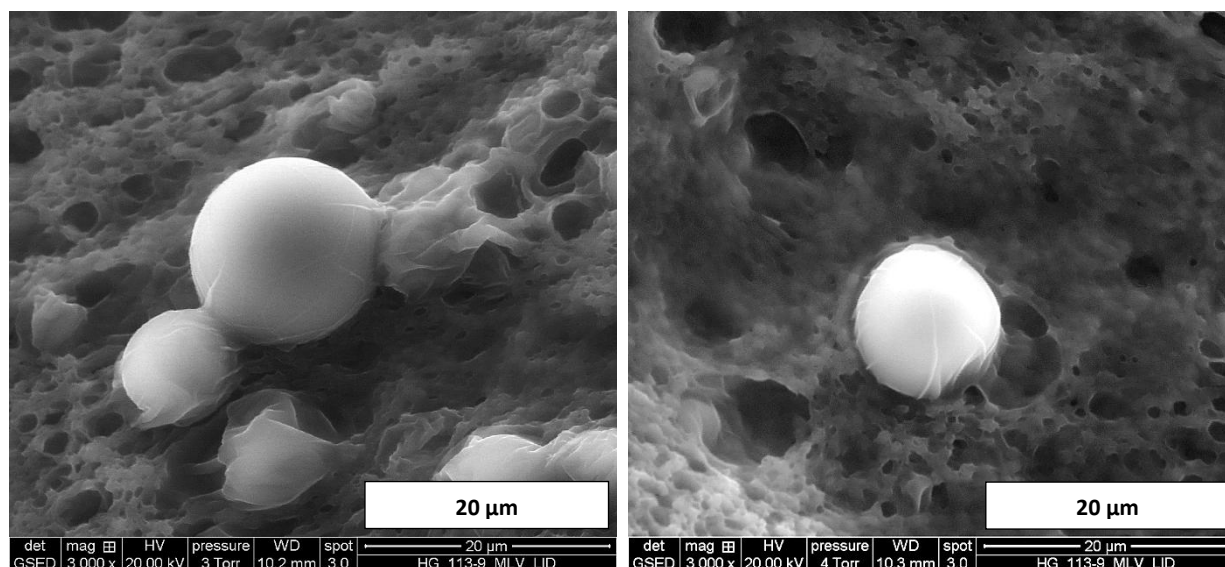


810

815 **Figure 3.** ESEM images of LID MLV-loaded CS hydrogels (DLH) at $t=0$ (A) and $t =$ after 2 minutes (B) at 3.5 Torr, and 5°C , showing that the smallest liposomes with highest curvatures disrupt the first in the ESEM chamber (a few examples are given in dotted circles as guide eyes) ($[\text{CS}] = 1.7\% \text{ w/w}$, $\text{DA} = 9\%$).

820

825



830

Figure 4. Examples of ESEM images at 3.5 Torr, and 5°C, showing the embedment of LID
835 MLV-type liposomes in the CS matrix of the hydrogel (DLH).

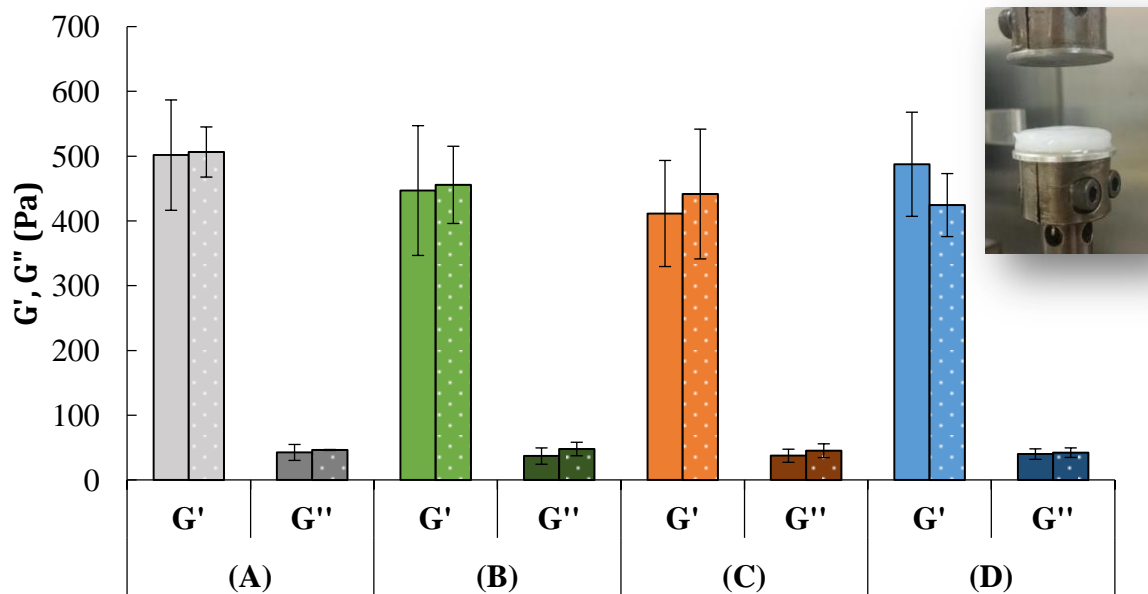
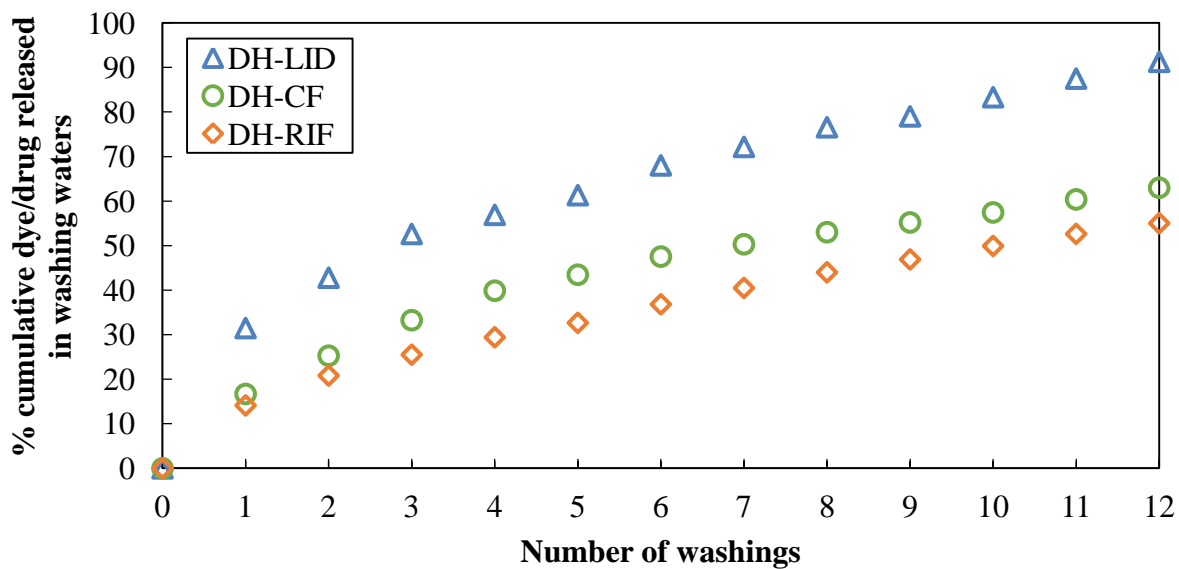


Figure 5. Variation of G'_{eq} and G''_{eq} moduli as a function of free dye/drug-loaded physical CS hydrogel (DH, filled bars) and dye/drug-loaded liposomes embedded into CS hydrogels (DLH, dotted bars) ($[CS] = 1.7\%$ w/w, $DA = 9\%$, lipid/CS mass ratio = 0.06 w/w). (A) Reference, no dye/drug, (B) CF, (C) RIF, (D) LID. Insert corresponds to an image of a DH assembly placed between the two plates of rheometer. $N \geq 3$ for each measurement, with N the number of measurements carried out on different hydrogels batches.

855

860

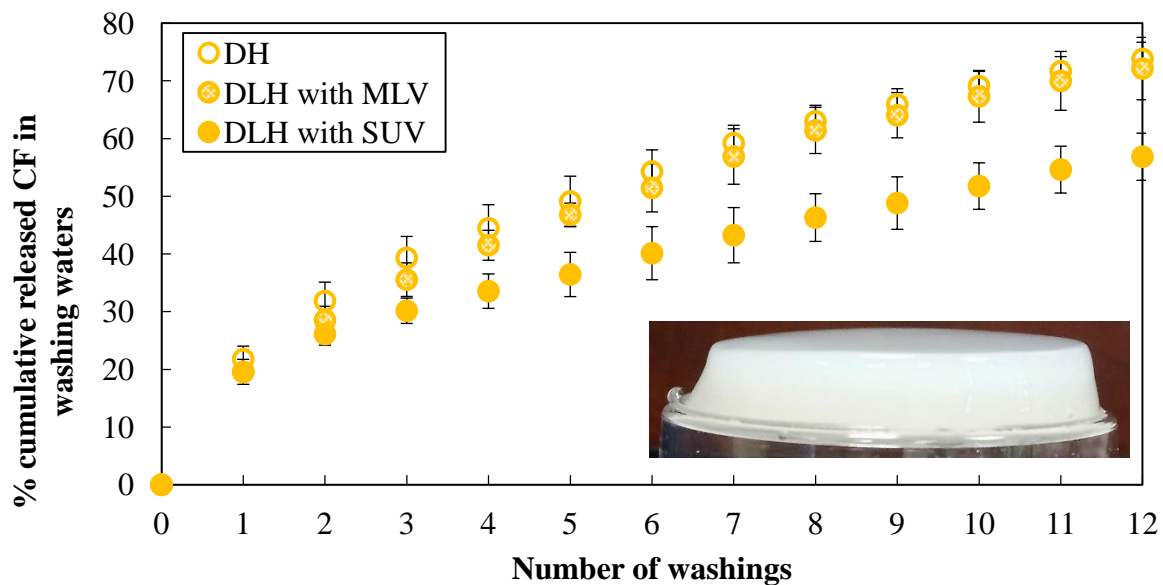


865

Figure 6. Dye/drug release profiles from DH assemblies containing initially $2.4 \cdot 10^{-6}$ mol per hydrogel of RIF (N=21, orange diamonds), LID (N=3, blue triangles) and CF (N= 1, green circles).

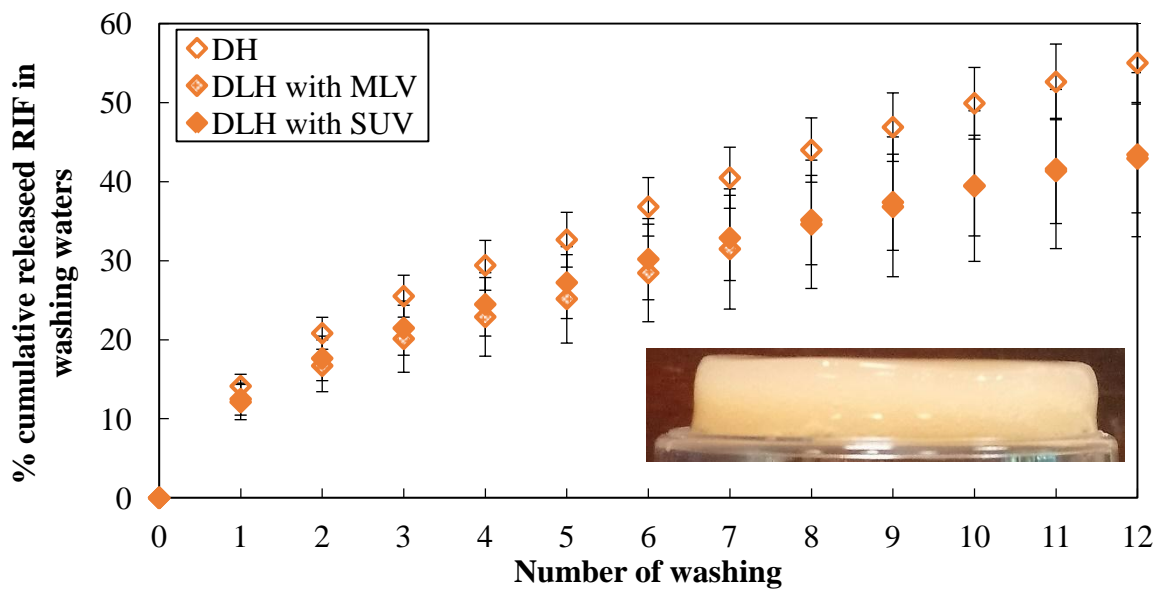
870

875



880

Figure 7. CF release profile from CS hydrogels containing CF ($[CF]_i = 10^{-4}$ M) without
885 liposome (empty circles, N=6) or CF loaded MLV (dotted circles, N=4) or -SUV (filled
circles, N=4). [CS] = 1.7%, DA = 9% (w/w). Inset corresponds to a photography of a CF-
DLH.

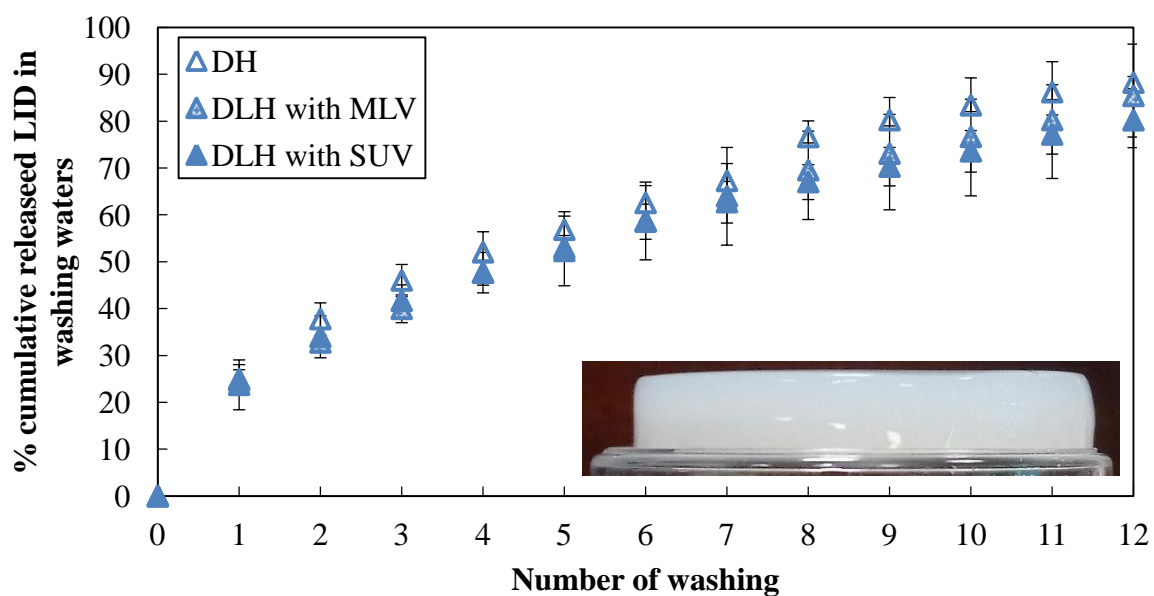


895

900 **Figure 8.** RIF release profile from CS hydrogels containing RIF ($[RIF]_i = 3.10^{-3}$ M) without liposome (empty diamonds, N=21), RIF loaded MLV (dotted diamonds, N=4) or -SUV (filled diamonds, N=21). [CS] = 1.7%, DA = 9% (w/w). Inset corresponds to a photography of a RIF-DLH.

905

910

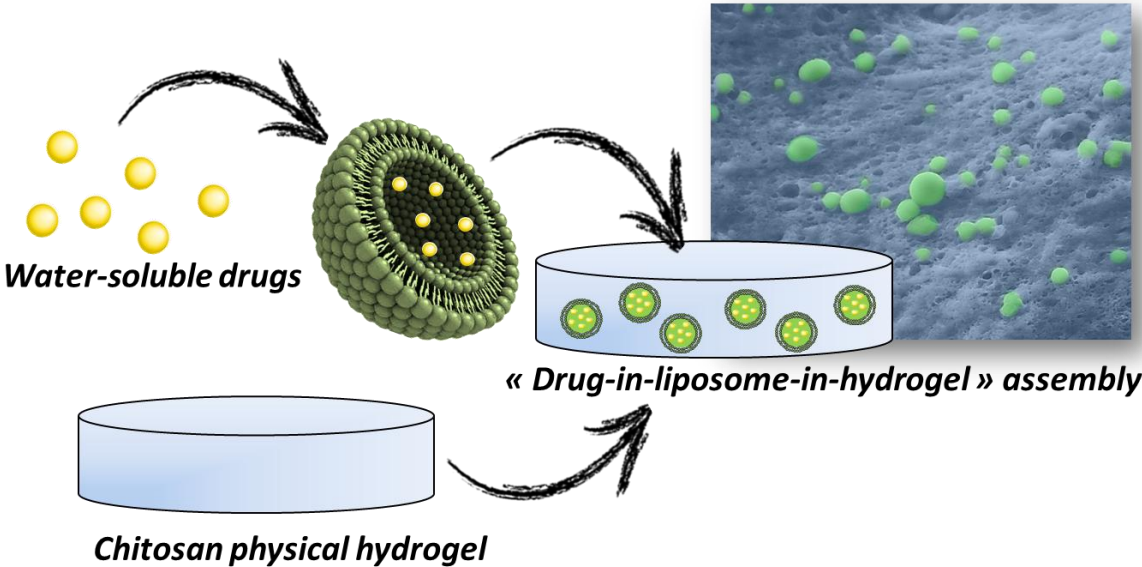


915

Figure 9. LID release profile from CS hydrogels containing LID ($[LID]_i = 3.10^{-2}$ M) without liposome (N=5), LID loaded MLV (N=1) or SUV (N=2). $[CS] = 1.7\%$, $DA = 9\%$ (w/w). Inset corresponds to a photography of a LID-DLH.

920

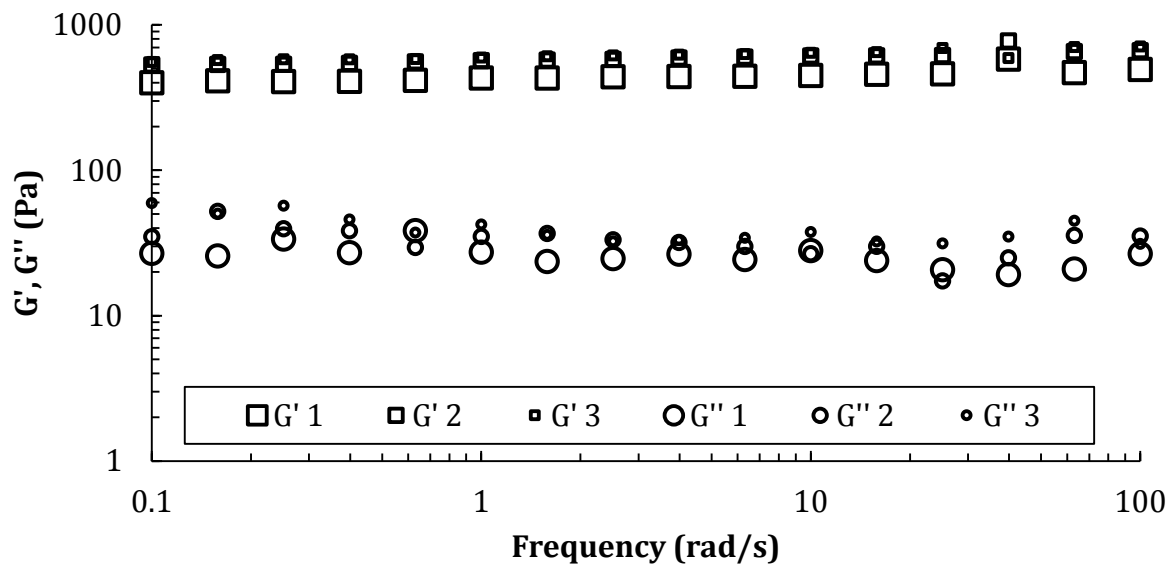
Graphical abstract - TOC



925

Supporting Information

930 Example of G' (squares) and G'' (circles) moduli variations versus frequency for three CS hydrogels without liposome, $[CS] = 1.7\%$ (w/w), $DA = 9\%$ at 25°C with a deformation of 1% .



Caption of Table

Table 1. Tan δ values of DH (free dye/drug loaded physical CS hydrogel) and DLH (dye/drug loaded liposomes embedded into CS hydrogels) assemblies. $N \geq 2$ for each measurement, with N the number of measurements carried out on different hydrogels batches ([CS] = 1.7% w/w).

Table 1. Tan δ values of DH (free dye/drug loaded physical CS hydrogel) and DLH (dye/drug loaded liposomes embedded into CS hydrogels) assemblies. $N \geq 2$ for each measurement, with N the number of measurements carried out on different hydrogels batches ([CS] = 1.7% w/w).

	tan δ			
	No dye/drug	CF	RIF	LID
DH assemblies	0.085	0.082	0.092	0.082
	± 0.015	$\pm 0,013$	$\pm 0,023$	± 0.010
	(N=3)	(N=7)	(N=11)	(N=6)
DLH assemblies	0.092	0.105	0.103	0.100
	± 0.006	± 0.019	± 0.011	± 0.020
	(N=2)	(N=3)	(N=5)	(N=3)

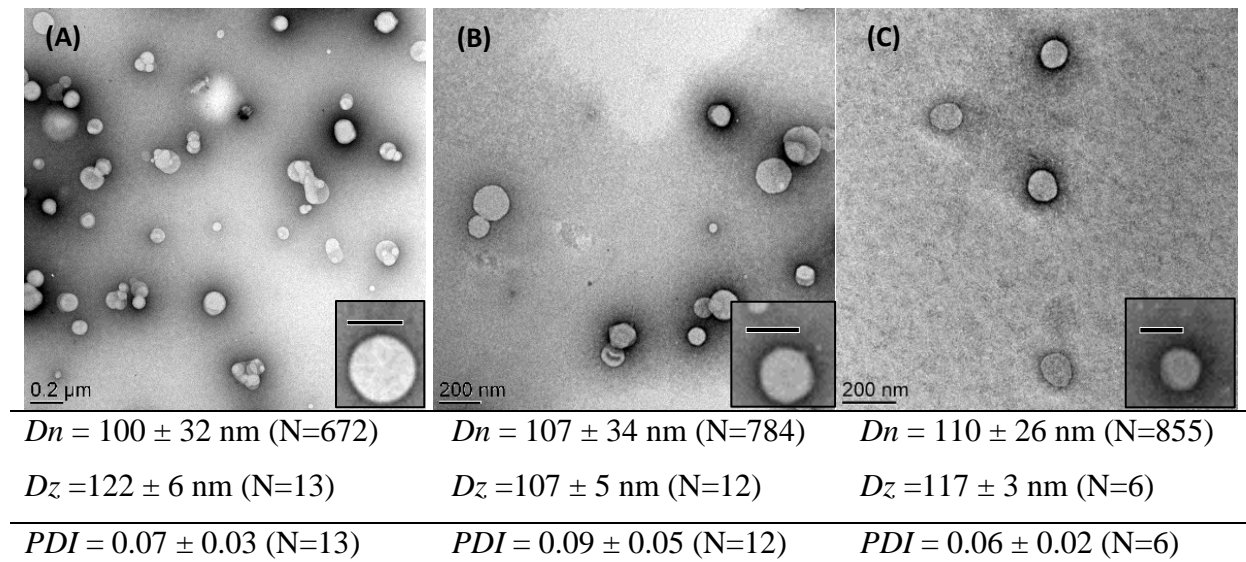
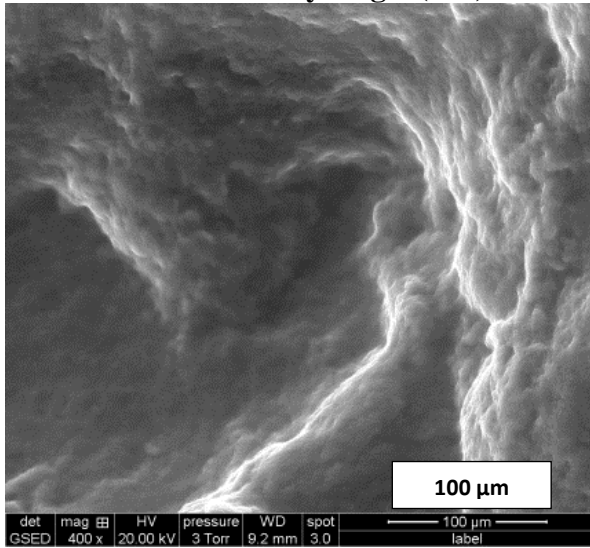
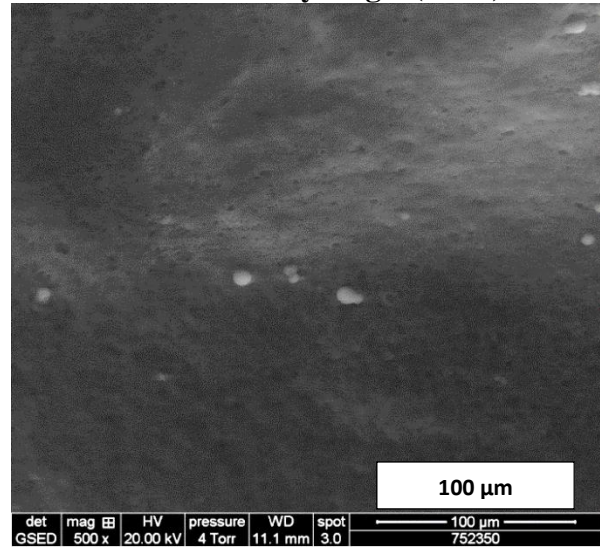


Figure 1. TEM images (with STS contrast agent at 1% w/w) and size characterization by TEM (using Image J, mean D_n) and DLS (mean D_z , PDI) of DPPC liposomal suspensions (SUV) incorporating CF (A), RIF (B) and LID (C). N is the measurement number. The scale bare in the insets are 125 nm.

**Dye/Drugs directly
inside the CS hydrogel (DH)**



**Dye/Drug-loaded MLV
inside the CS hydrogel (DLH)**



Sample
holder

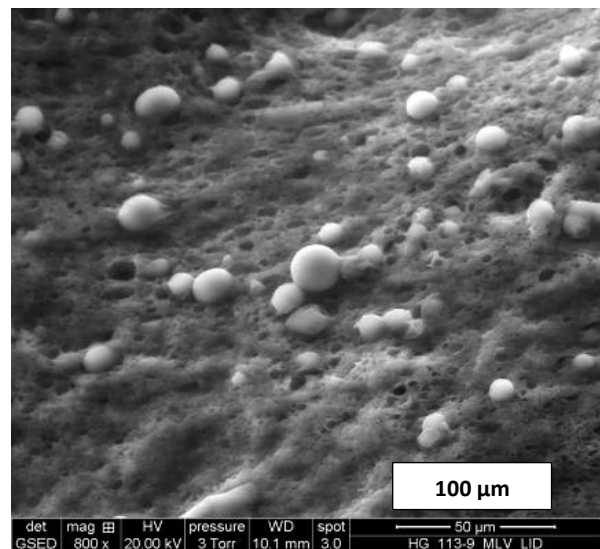
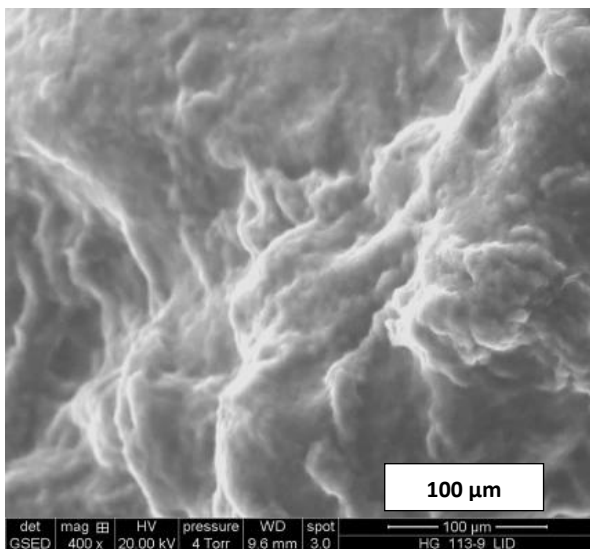
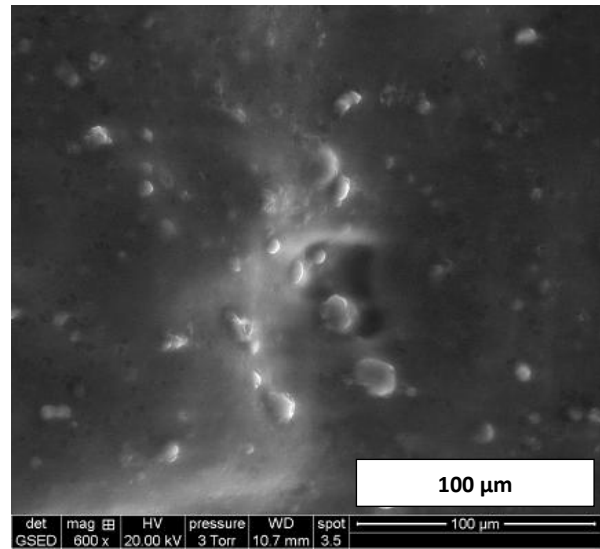
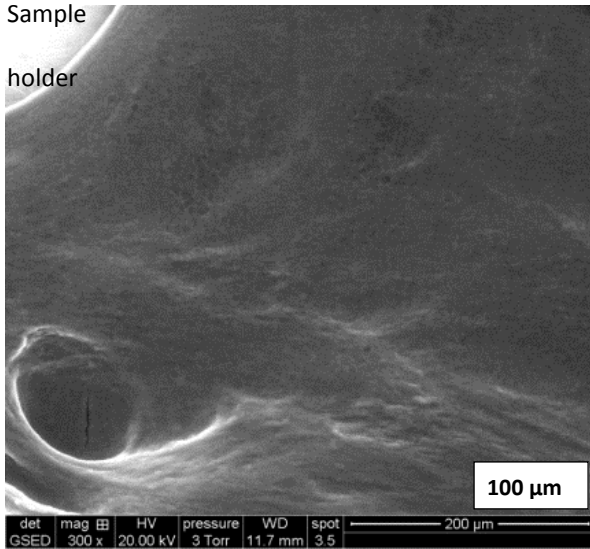


Figure 2. ESEM images at the left-hand column: DH with (A) CF, (B) RIF, (C) LID (without liposome), at the right-hand: DLH with (A) CF, (B) RIF, (C) LID/MLV-loaded, at 3.5 Torr and 5°C after 12 washings ([CS] = 1.7% w/w, DA = 9%).

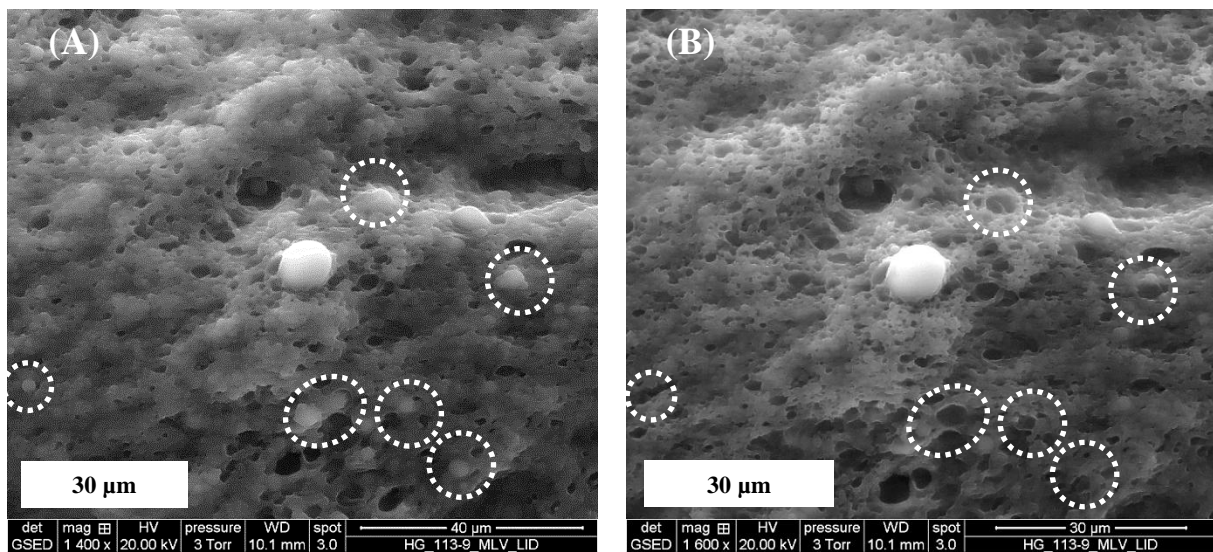


Figure 3. ESEM images of LID MLV-loaded CS hydrogels (DLH) at $t=0$ (A) and $t =$ after 2 minutes (B) at 3.5 Torr, and 5°C , showing that the smallest liposomes with highest curvatures disrupt the first in the ESEM chamber (a few examples are given in dotted circles as guide eyes) ($[\text{CS}] = 1.7\% \text{ w/w}$, $\text{DA} = 9\%$).

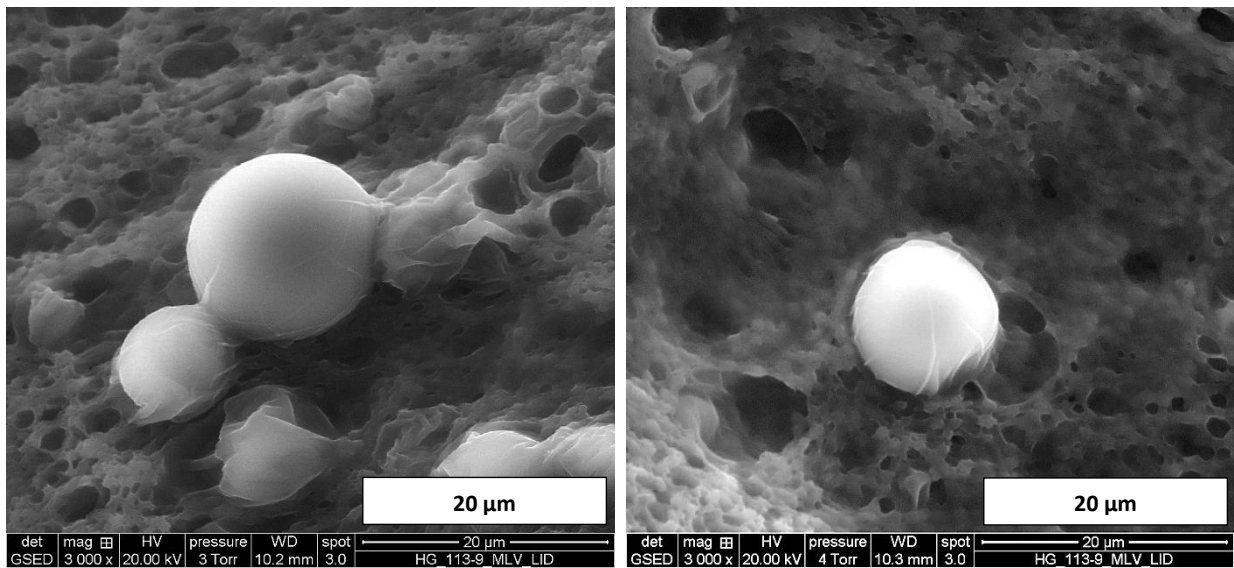


Figure 4. Examples of ESEM images at 3.5 Torr, and 5°C, showing the embedment of LID MLV-type liposomes in the CS matrix of the hydrogel (DLH).

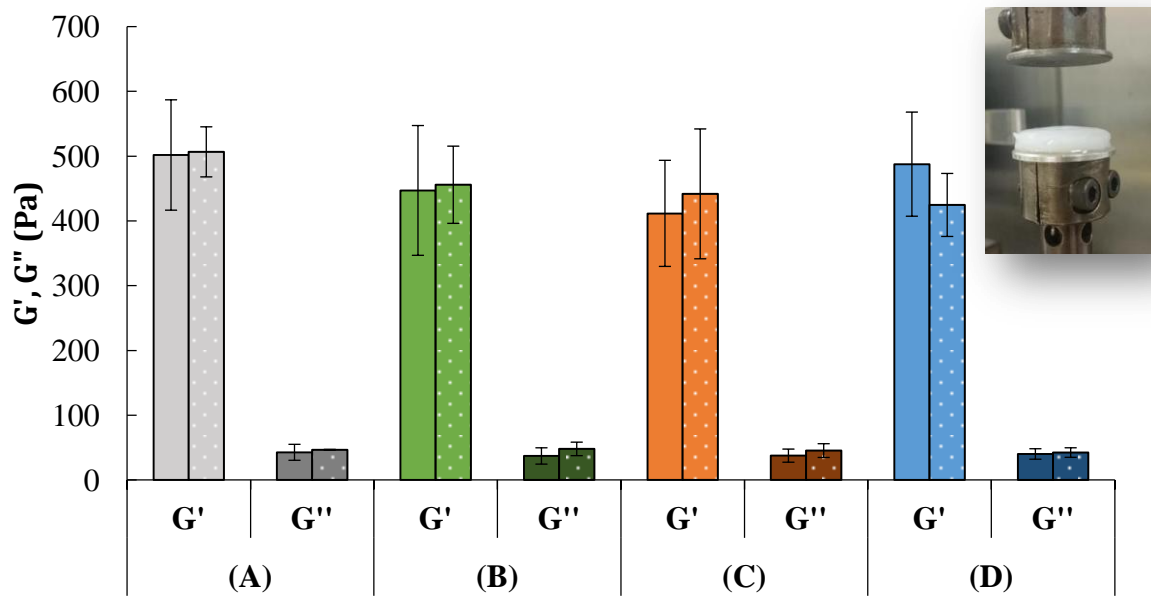


Figure 5. Variation of G'_{eq} and G''_{eq} moduli as a function of free dye/drug-loaded physical CS hydrogel (DH, filled bars) and dye/drug-loaded liposomes embedded into CS hydrogels (DLH, dotted bars) ($[CS] = 1.7\%$ w/w, $DA = 9\%$, lipid/CS mass ratio = 0.06 w/w). (A) Reference, no dye/drug, (B) CF, (C) RIF, (D) LID. Insert corresponds to an image of a DH assembly placed between the two plates of rheometer. $N \geq 3$ for each measurement, with N the number of measurements carried out on different hydrogels batches.

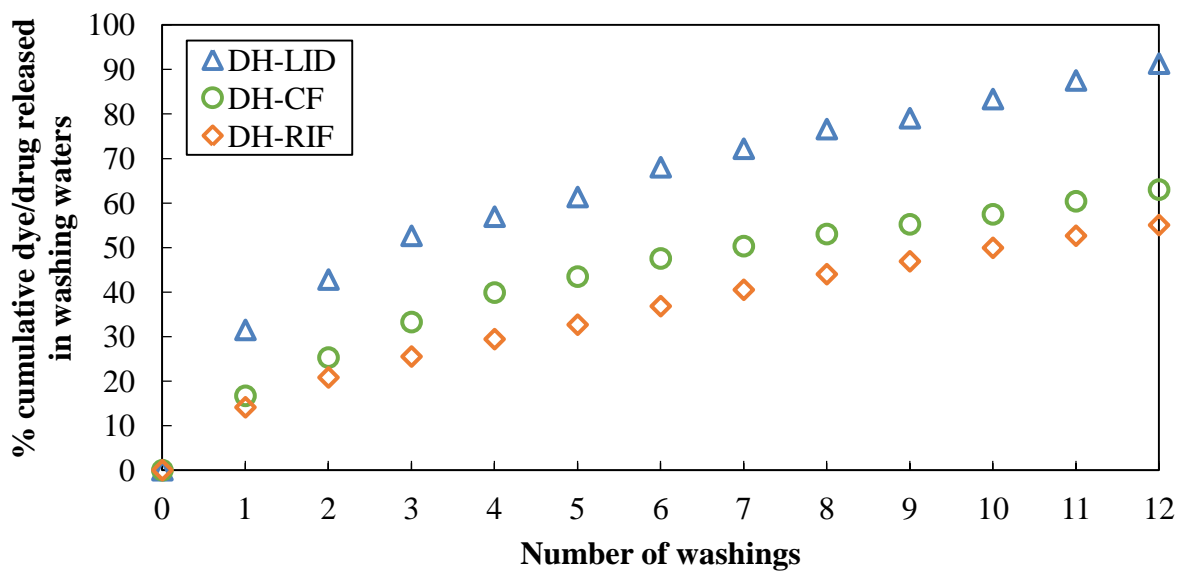


Figure 6. Dye/drug release profiles from DH assemblies containing initially $2.4 \cdot 10^{-6}$ mol per hydrogel of RIF (N=21, orange diamonds), LID (N=3, blue triangles) and CF (N= 1, green circles).

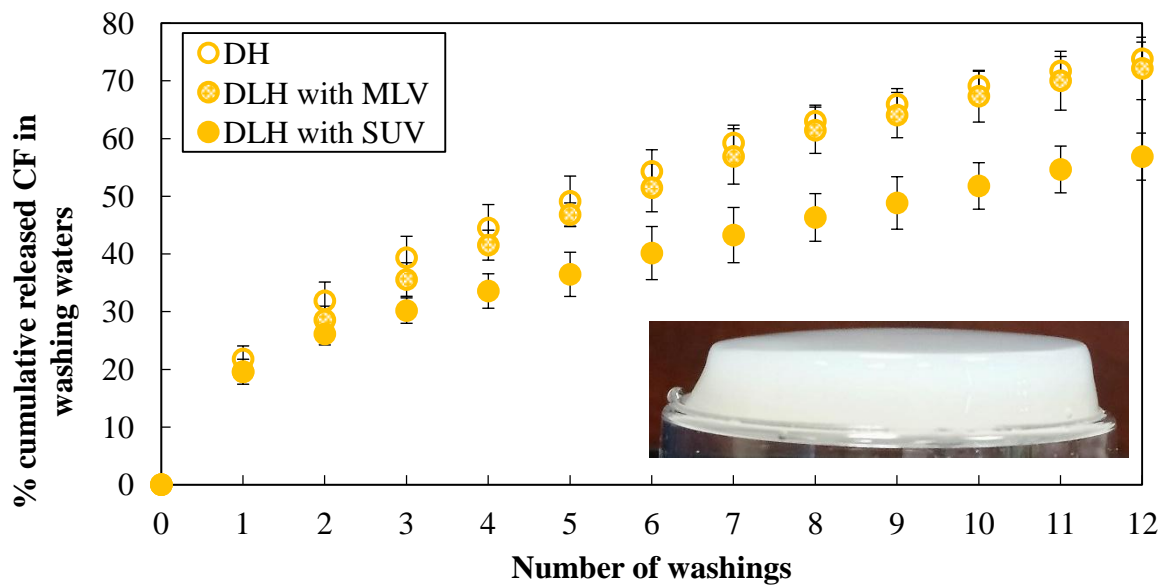


Figure 7. CF release profile from CS hydrogels containing CF ($[CF]_i = 10^{-4}$ M) without liposome (empty circles, N=6) or CF loaded MLV (dotted circles, N=4) or -SUV (filled circles, N=4). $[CS] = 1.7\%$, $DA = 9\%$ (w/w). Inset corresponds to a photograph of a CF-DLH.

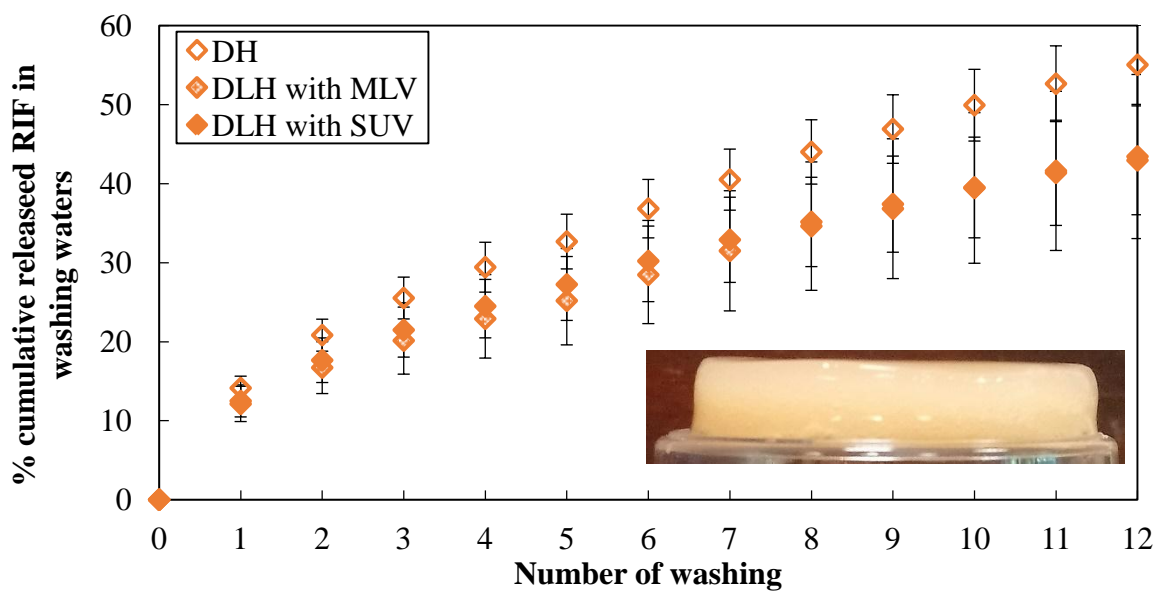


Figure 8. RIF release profile from CS hydrogels containing RIF ($[RIF]_i = 3.10^{-3}$ M) without liposome (empty diamonds, N=21), RIF loaded MLV (dotted diamonds, N=4) or -SUV (filled diamonds, N=21). [CS] = 1.7%, DA = 9% (w/w). Inset corresponds to a photography of a RIF-DLH.

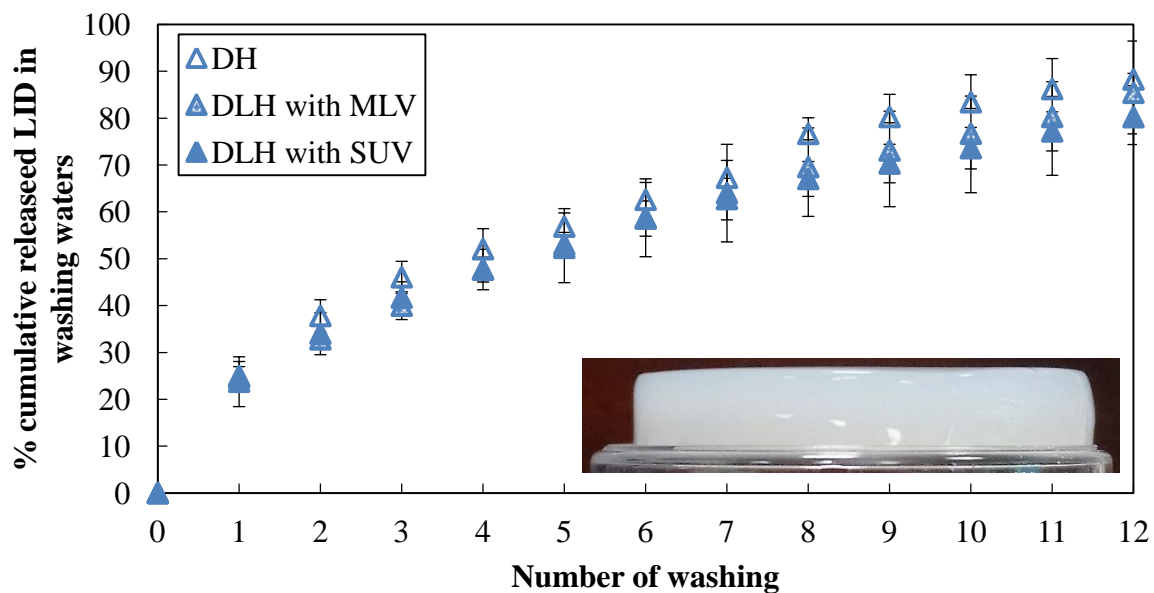


Figure 9. LID release profile from CS hydrogels containing LID ($[LID]_i = 3.10^{-2}$ M) without liposome (N=5), LID loaded MLV (N=1) or SUV (N=2). $[CS] = 1.7\%$, $DA = 9\%$ (w/w). Inset corresponds to a photography of a LID-DLH.

Supplementary data

[Click here to download Supplementary data: SI_Embedment of liposomes into CS phys HG_S Peers.docx](#)